Original Article

Retinal Protective Effect of Avocado Soybean (ASB) Versus Glibenclamide in Streptozotocin- Induced Diabetic Rats

Rasha Salama[1] and Seham Ahmed Mohammed Abdelaziz[2]

[1]Department of Anatomy and Embryology, [2]Department of Histology and Cell Biology, Faculty of Medicine, Menoufia University, Egypt

ABSTRACT

Introduction: Diabetic retinopathy is a neurodegenerative, microvascular, and sight-threatening impact of chronic uncontrolled diabetes. Avocado/soybean (ASB), a relatively new nutraceutical mixture, has acquired a significant role as a natural substitutional therapy for numerous diseases. Glibenclamide (Gli), a potent sulfonylurea, was confirmed as a diabetic therapy.

Aim of the Study: To explore the protective effects of ASB versus glibenclamide on the diabetic rats' retina induced by streptozotocin (STZ).

Materials and Methods: Forty rats were categorized into four groups: Normal control, Diabetic Control, Diabetes+Avocado soybean, and Diabetes+Glibenclamide. Retinal specimens were processed for histological, immunohistochemical, ultrastructural studies. Morphometrical and statistical studies were also performed.

Results: Diabetic retinal specimens demonstrated evident disorganization of the retinal layers, degenerated retinal pigment epithelium, photoreceptors, and outer nuclear layers with appearance of empty spaces and multiple vacuolations. Most of ganglion cells were lost, others appeared with pycnotic nuclei. Together with a highly significant decrease ($P< 0.001$) of the total thickness, and the thickness of the outer and inner nuclear layers of the rats' retina, and the number of the ganglion cells. Immune expression of TNF-α, VEGF, caspase-3, and vimentin illustrated a highly significant elevation ($P< 0.001$). Ultrastructural findings of retinal pigmented cell layer illustrated; swollen degenerated mitochondria with cytoplasmic vacuolation. Degenerated photoreceptors, ganglion cells have indented irregular nucleus, destructed nuclear membrane, and vacuolated cytoplasm. ASB amends the diabetic retinopathy changes, structurally and immunohistochemically, more than glibenclamide

Conclusion: ASB has a more, retinal-protective efficacy on DR, than glibenclamide.

Received: 03 September 2022, **Accepted:** 15 November 2022

Key Words: Avocado/soybean, caspase 3, diabetic retinopathy, glibenclamide, TNF-α, VEGF, vimentin.

Corresponding Author: Seham Ahmed Mohammed Abdelaziz, MD, Department of Histology and Cell Biology, Faculty of Medicine, Menoufia University, Egypt, **Tel.**: +2 04 8400449, **E-mail:** dr.sehamhist@gmail.com

ISSN: 1110-0559, Vol. 47, No. 1

INTRODUCTION

Retina is the sensory neuro-integrated layer of the orbit. It is the most complex structure and considered as a special area of the brain. Retinal ganglion cells (RGCs) are the final common pathway neurons of the retina and therefore are of critical importance to the visual system[1]. Therefore, retinal diseases mostly end with diminished sight and blindness[2].

Diabetic retinopathy (DR) is a progressive sight-threatening impact of uncontrolled diabetes mellitus (DM) and is the commonest reason of vision loss in the United States between 24-75 years-old. An estimated universal expansion of DR will be 191.0 million by 2030, among them 56.3 million proceeding to sight-threatening manifestations[2]. DR is the most common microvascular complications of DM, displaying a dynamic process to proliferative retinopathy from non-proliferative retinopathy[3].

The pathophysiology of DR is complicated, in addition to the documented vascular alterations as, hemorrhages, vascular leakage, microaneurysms, and neovascularization, also it influences neural components of the retina[4].

Cumulation of tissue macromolecules during hyperglycemia progressively created advanced glycation end products by non-enzymatic glycation[5], that results in microvascular lesions; including microaneurysms, blood barrier dysfunction, and endothelial cell dysfunction[6]. Also, basement membrane thickening that leads to vascular wall insufficiency and raised permeability of the blood-retinal barrier (BRB) causing diabetic leakage and edema of the macula[7,8].

Vascular permeability rises capillary obstruction leading to ischemia of the retina, and inducing an elevation of VEGF expression, afterwards neovascularization was promoted[7,8]. Many studies support the pivotal inflammatory and neurodegenerative changes in the pathogenesis and development of DR[9,10,11], including a previous study, when cells were drenched in a rich-glucose medium for some time, a process called metabolic memory happened where previous high-glucose exposure, could

 DOI: 10.21608/ejh.2022.164735.1779

not fully inhibit the inflammatory response even with controlling diabetes[12].

Many therapeutic approaches to DR have been found to be partly successful comprising; laser treatment, and vitreous cut surgery[13], While first-line therapies as intra-vitreal steroids and anti-VEGF components were successful against DR inflammation and angiogenesis[14,15]. These therapies remain unattractive due to their invasive mode of application, inability to prohibit progression of early to late retinopathy stages, in addition to its high cost[16].

Hence, early interference by new approaches is of magnificent importance to counteract the progression of DR, and the vision loss associated with it.

Glibenclamide (Gli), a potent sulfonylurea, was approved as a type II DM therapy thirty-eight years ago. Gli, acts by closing ATP-sensitive potassium channels (KATP) that was found in pancreatic β-cells leading to cells depolarization and insulin secretion[17].

In growing countries, traditional curative plants were consumed by 80% and more of the population. It was accepted as a complementary medicine to treat a variety of diseases and improve the health condition through counteracting adverse effects and prices of the synthetic medicines[18].

From this point, finding and utilizing beneficial medicinal plants, and their constituents instead of synthetic medicines against retinopathy, is very essential.

For example, Avocado/soybean (ASB), a relatively new nutraceutical mixture, that is increasing in popularity, it consists of the oil fractions of avocados and soybeans in a ratio of 1:2, this mixture is prescribed as an adjuvant therapy for osteoarthritic pain, hip and knee osteoarthritis, rheumatoid arthritis and autoimmune disorders. Additionally, it was recommended for postmenopausal women to improve the mood[19]. Studies have reported ASB anti-inflammatory and proliferative effects by downregulating the production of iNOS, TNFα, IL1β, IL6, and IL8 pro-inflammatory mediators[20].

In the current study, we were seeked to explore the protective effects of ASB versus glibenclamide on the diabetic rats' retina induced by streptozotocin (STZ).

MATERIAL AND METHODS

Chemicals

Streptozotocin (STZ): was obtained from (Sigma Aldrich, Egypt) as a vial containing 1.5 g powder of STZ and 220 mg citric acid, it was dissolved in 0.1 M sodium citrate buffer and used freshly within 5 minutes of preparation.

Avocado Soybean (Avosoya, Trend pharm company, Egypt): was obtained from a pharmacy. The capsule has 100 mg and 200 mg avocado oil and soya bean oil respectively. The experimental dose is 27.5 mg/kg/day (equal to 300 mg/day dose in humans) dissolved freshly in 1 M distilled water and given orally for 14 days[21].

Glibenclamide (Daonil, Sanofi Aventis, Egypt): was obtained from a pharmacy. The tablet has 5 mg glibenclamide. The experimental dose is (2.5 mg/kg) dissolved freshly in 1 M distilled water and given orally for 14 days[22].

Induction of diabetes

Streptozotocin (STZ, Sigma, USA) was solved in 0.02 M citrate buffer (pH 4.5) and kept on ice then immediately used. In order to access the appropriate dose, each rat was weighed before injection. One intraperitoneal injection of STZ (60 mg/kg) was given to fasted rats to induce diabetes. After injection, the rats received 5 M solution of glucose for 12 hours to prevent reducing of blood glucose. About 72h later, level of fasting blood glucose was estimated by obtaining blood from the tail and using one touch glucometer, and when blood glucose levels were more than 16.7 mmol/L (300 mg/dl), animals were assumed to have diabetes[23].

Animals

Forty adult male albino rats weighing 220-240 g (3-5 months old) were resident at the animal house of Medical Research Institute, Alexandria University, Egypt. They were maintained under standard lab conditions (five rats in per cage, ambient temperature of 23 ± 2°C, with a 12-hour light/dark cycle and unrestricted access to food and drink). All experiment was done in conjugation with the health rules for the use of animals that prepared by the University Ethics and Committee (No: 9/2022 HIST 8), Faculty of Medicine, Menoufia University.

Experimental design

After one-week adaptation, the forty rats were categorized into four groups (n= 10 per group).

Group 1, Normal control (NC): Rats subdivided into two subgroups (n= 5 per subgroup)

- Subgroup 1a: Rats received standard diet and ordinary drinking water.
- Subgroup 1b: Rats received 0.02 M citrate buffer as a single intraperitoneal injection (vehicle of STZ).

Group 2, Diabetic Control (DC): to induce diabetes, rats received STZ (60mg/kg, b.w) as a single intraperitoneal injection.

Group 3, Diabetes Avocado soybean (DM+ASB): Rats that developed diabetes 72 h after STZ injection, received ASB (27.5 mg/kg/day) daily orally by gavage[21].

Group 4, Diabetes+Glibenclamide (DM+Gli): Rats that developed diabetes 72 h after STZ injection, received Gli (2.5 mg/kg) daily orally[22].

After 14 days, ether inhalation (2 ml) was utilized for the rats for about 2 minute[24] and sacrificed by cervical decapitation, and both eyeballs were enucleated from all rat groups.

Histological, Immunohistochemical and Electron microscopic studies

For histological and immunohistochemical studies, the right eyeballs were injected with 10% formalin and for electron microscopic study, the left ones were injected with 5% phosphate buffered glutaraldehyde.

light microscopic study, retinal tissue sections from right eyeballs of all rat groups were dehydrated, cleared, and embedded in paraffin wax. A rotating microtome was used to cut 5-7 µm sections, and subjected to:

I. Histological study, Hematoxylin and Eosin (H&E) and Toluidine blue stains[25]. Slides were observed using light microscope for diagnosis of retinal histology and morphology.

II. Immunohistochemical study:

1. Tumor necrosis factor alpha, TNF-α (for detection of inflammation): primary monoclonal antibody utilized was the mouse anti-TNF-α (1:300 with PBS). Cells appeared with brown cytoplasm. tonsil was used as appositive control for anti-TNF.

2. Vascular Endothelial Growth Factor, VEGF (angiogenesis index): primary monoclonal antibody (1:200; sc-152) used was the goat polyclonal antibody (Santa Cruz Company, California, USA) (1:500 with PBS). The cellular site of the reaction was cytoplasmic brown in color. Colon and Placenta adenocarcinoma were used as a positive control.

3. Caspase-3 (marker for apoptosis): Anti-Caspase-3 (rabbit polyclonal antibody, Thermo Science, Fermont, CA 94539, USA at a dilution 1/50) was used. The primary antibody used was ready-to-use rabbit polyclonal antibody (CAT-No. RB-3425-R2). The cellular site of the reaction was brown cytoplasmic color. Normal lymphoid tissue was used as a positive control for caspase-3.

4. Vimentin (index for gliosis): primary monoclonal mouse antibody for Vimentin (Santa Cruz Biotechnology, Santa Cruz, California, USA, 1:300 wits PBS) was used to detect the whole Müller cells. cytoplasmic brown color was the cellular site of the reaction, the positive control was smooth muscle tissue.

Mayer's hematoxylin was used to counter-stain sections later. Negative controls stained with PBS alone, substituting the primary antibody[26,27].

Electron microscopic study, the left eye from all rat groups where processed, and epoxy resin embedded by routine protocol. Semithin sections (1 µm thick) were obtained and 1% toluidine blue stained followed by light microscopy inspection. on copper grids, ultrathin retinal sections (80-90 nm) were mounted, before being stained with uranyl acetate as well as lead citrate. Examination of the grids of the retinal specimens was done by using Jeol electron microscope (Seo-Russia) in electron microscopic unit, Faculty of Medicine, Tanta University[28].

Morphometrical study

Image analysis computer system (Leica Qwin 500 C Image analyzer computer system; Leica Imaging System LTD., Cambridge, England) was used at the histology department, Faculty of Medicine, Menoufia University to measure the parameters. Ten different fields at a magnification of 400 were examined in each slide for:

1. Total thickness of the rats' retina and the thickness of its outer and inner nuclear layers (H&E-stained sections).

2. Number of the ganglion cells (per 100 µm length of the ganglion cell layer) (H&E-stained slides).

3. Areapercentage(area%)ofTNF-α,VEGF,vimentin, and caspase-3 positive immunohistochemical reaction (Immunohistochemical stained slides).

Statistical analysis

SPSS (version 20, SPSS Inc., Illinois, Chicago, USA) was used to categorize, and analyze the data. Quantitative information that was gathered was summarized as mean, standard deviation and range. Mann Whitny U test was done to compare each two groups that were being researched. *P value* <0.05 was statistically significant.

RESULTS

The two subgroups of Group 1 (NC) showed similar histological, immunohistochemical, electron microscopic, morphometrical, and statistical analysis results over all the studied parameters. So, Group 1 applied to them.

light microscopic histological results

a) Hematoxylin and Eosin stain results

Group 1, Normal Control (NC), illustrated well organized histological architecture of the retinal layers from outside inwards are retinal pigment epithelium (RPE), clarified as a single layer of low cuboidal cells with flat nuclei, photoreceptor layer (PRL) established of outer and inner segments of rod and cone cells, outer limiting membrane seemed as dark line, outer nuclear layer (ONL) comprised of several rows of the bodies of rods and cones with their densely stained nuclei, outer plexiform layer (OPL) clarified as a small pale area, inner nuclear layer (INL) seemed with larger and paler nuclei than ONL, inner plexiform layer (IPL) has a thick pale eosinophilic fibrillary appearance, ganglion cell layer (GCL) composed of a single row of ganglion cells displaying enormous light stained cytoplasm, vesicular spherical or angular

nuclei with prominent nucleoli and nerve fiber layer (NFL) formed of axons of GCL, and inner limiting membrane seemed as dark line that distinguishing retina from vitreous body (Figures 1A, 2A).

Group 2 (Diabetic Control), demonstrated marked disorganized layers of the retina, degenerated RPE, photoreceptors, and ONL with appearance of empty spaces between the nuclei of ONL, INL and GCL. Multiple vacuolation within ONL, INL, IPL, and GCL. OPL showing disruption. INL exhibited pycnotic nuclei. Ganglion cell layer showed a large congested blood vessel, that extends to inner plexiform layer. Also, most of ganglion cells were lost, others appeared with pycnotic nuclei (Figures 1,2B,2C).

Group 3 (Diabetes+Avocado soybean) demonstrated retinal layers, more or less like control group, formed of well-organized PRL, outer limiting membrane, ONL, OPL, INL, IPL, GCL, NFL and inner limiting membrane. With appearance of the Muller's cells supporting fibers (Figures 1C, 3A). While Group 4 (Diabetes+Glibenclamide) showing improvement in some retinal layers including, PRL, ONL, and OPL. However, there is degenerated RPE and some photoreceptor layer, together with small capillary within INL, vacuolation within INL, IPL, GCL. Also, there is congested blood vessel and pycnotic nuclei within ganglion cell layer (Figures 1D, 3B).

b) Toluidine blue stain results

Group 1 (Normal Control) displayed the different layers of the retina. RPE layer cells appear as a single row of cuboidal cells. The PRL appeared as elongated barrel-shaped structures. ONL is formed of several layers of the rods and cones cell bodies with their scanty cytoplasm and dark nuclei. The processes of these cells extend into OPL. INL contains large cells and pale nuclei than those in the ONL. INL layer comprised of four cell types: bipolar cells, horizontal cells, muller cells, and amacrine cells. IPL is thicker than the OPL. GCL revealed a single layer of light stained cytoplasm and pale nuclei with prominent nucleoli of ganglion cells and darkly stained nuclei of astrocytes. Also, inner limiting membrane seen as a dark stained line (Figure 4A).

Group 2 (Diabetic Control) illustrated the photoreceptor layer filled with multiple empty spaces. ONL appeared with dark stained nuclei, OPL showed marked thinning. INL showed widely separated nuclei, cytoplasmic vacuolation, many blood capillaries, and many Muller cells. GCL revealed total degeneration and lysis of ganglion cells cytoplasm with dissolution of their nuclei, and appearance of congested blood vessel (Figure 4B).

Group 3 (Diabetes+Avocado soybean) showed the different retinal layers more or less identical to control (Figure 4C). While Group 4 (Diabetes+Glibenclamide) still displayed vacuolation within ONL, INL and GCL. Some ganglion cells are lost (Figure 4D).

light microscopic immunohistochemical results

a) Tumor Necrosis Factor-α (TNF-α)

TNF-α immunohistochemical stained section of the retina of Group 1; demonstrated a very weak cytoplasmic intensity in all layers (PL, ONL, OPL, INL, IPL and GCL) (Figure 5A). Group 2; demonstrated a strong positive high intensity immune reaction in ONL, OPL, INL, IPL, and GCL layers (Figure 5B). Group 3; demonstrated a weak intensity immune reaction in GCL layer only (Figure 5C). However, Group 4; demonstrated a moderate intensity immune reaction in INL, IPL, and GCL layers of the retina (Figure 5D).

b) Vascular endothelial growth factor (VEGF)

VEGF immunohistochemical stained section of Group 1; illustrated a negative immunoreaction in ONL, OPL, INL, IPL, and GCL layers of the retina (Figure 6A). Group 2; illustrated a strong positive cytoplasmic immunoreaction intensity in INL, IPL, and GCL layers of the retina (Figure 6B). Group 3; illustrated a very weak immunoreaction intensity in INL layer only (Figure 6C). However, Group 4; illustrated a moderate immunoreaction intensity in INL, IPL, and GCL layers of the retina (Figure 6D).

c) Caspase-3

Caspase-3 immunohistochemical stained section of retina of Group 1; demonstrated a very weak cytoplasmic immune reaction in ONL, OPL, INL, IPL, and GCL layers of the retina (Figure 7A). Group 2; demonstrated a strong positive high intensity immune reaction for caspase-3 in ONL, INL and GCL layers (Figure 7B). Section of Group 3; showed a week intensity caspase-3 immune reaction in INL layer only (Figure 7C). However, Group 4 showed a moderate intensity caspase-3 immune reaction in ONL and INL layers (Figure 7D).

d)Vimentin

Vimentin immunohistochemical stained section of the retina of Group 1; showed a very weak immunoreactivity in the Muller cell end feet and Muller fibers found in IPL and GCL layers (Figure 8A). Group 2; showed a strong positive immunoreactivity in ONL, OPL, INL, IPL, and GCL layers of the retina (Figure 8B). Section of Group 3; showed a weak immunoreactivity in the Muller cell end feet and Muller fibers in OPL, INL, IPL and GCL layers (Figure 8C). However, Group 4; demonstrated a moderate immunoreactivity in ONL, OPL, INL, IPL and GCL layers (Figure 8D).

Transmission electron microscopic results

Group 1 (Normal Control), demonstrated retinal pigment epithelial cell layer having large euchromatic oval nucleus, cisterna of rough endoplasmic reticulum, mitochondria, melanin granules, long apical microvilli and phagocytosed photoreceptors outer segments (Figure 9A). The outer segments photoreceptors appeared

as long, straight, cylindrical structures containing regular flat horizontal lamellar discs (Figure 10A). Outer nuclear layer appeared with rounded centrally located nuclei with highly condensed heterochromatin, enveloped by a thin rim of cytoplasm and mitochondria. Cells are tightly backed with no intercellular spaces (Figure 11A). INL showed the bipolar cells cell bodies, tightly packed to each other and having euchromatic rounded nuclei, rounded or elliptical in shape and enveloped by thin rim of cytoplasm filled with mitochondria. Muller cells contain nuclei of high density (Figure 12A). Ganglion cell having large rounded euchromatic nucleus with intact nuclear envelope surrounded by thin rim of cytoplasm containing mitochondria, rough endoplasmic reticulum and scattered ribosomes (Figure 13A).

Group 2 (Diabetic Control), illustrated retinal pigmented cell layer resting on Bruch's membrane with destructed disturbed apical microvilli, small darkly stained nucleus and swollen degenerated mitochondria with destructed cristae. The cytoplasm displayed large phagosomes and vacuolization (Figure 9B). Multiple photoreceptors outer segments are separated by wide spaces. Some of these outer segments are degenerated, others showed vacuolation and distorted lamellar discs (Figure 10B). ONL showed cells with dark stained nuclei, others with cytoplasmic vacuolization. The nuclei are disconnected by wide intercellular spaces with debris (Figure 11B). Inner nuclear layer cells having condensed nuclei, swollen degenerated mitochondria with distorted cristae, many cytoplasmic vacuolization, and dilated rough endoplasmic reticulum (Figure 12B). In the GCL, ganglion cell appeared with indented irregular nucleus, and destructed nuclear membrane. The cytoplasm is vacuolated, together with presence of congested blood capillary (Figure 13B).

Group 3 (Diabetes+Avocado soybean), demonstrated an organization more or less like control. Where, the retinal pigment epithelial cell layer appeared resting on Bruch's membrane, having euchromatic oval nucleus, mitochondria, melanin granules and long apical microvilli (Figure 9C). Also, there is improved photoreceptors outer segments with intact regular flattened horizontal lamellar discs (Figure 10C). The outer nuclear layer showed rounded centrally located nuclei surrounded by mitochondria. Small area of the outer plexiform layer can be seen having intact nerve axons and containing mitochondria (Figure 11C). INL showed the bipolar cells cell bodies, tightly packed to each other and having euchromatic rounded nuclei, and smooth contour of mitochondria (Figure 12C). Ganglion cell having large rounded nucleus surrounded by thin rim of cytoplasm containing mitochondria, and nearly normal rough endoplasmic reticulum (Figure 13C). However, Group 4 (Diabetes+Glibenclamide), showed retinal pigment epithelial cell layer, resting on Bruch's membrane separating it from the chorio-capillary layer, having euchromatic oval nucleus, mitochondria, melanin granules and phagocytosed photoreceptors outer segments. But still there are degenerated microvilli, and large phagosomes (Figure 9D). There are some improved photoreceptors outer segments with regular flattened horizontal lamellar discs, but some segments still showing vacuolation and distorted lamellar discs (Figure 10D). The outer nuclear layer appeared with rounded centrally located nuclei but there are cytoplasmic vacuolation and the nuclei are separated by wide intercellular spaces. (Figure 11D). The inner nuclear layer demonstrated bipolar cells with euchromatic rounded nuclei, some mitochondria are normal others are degenerated, and cytoplasmic vacuolation (Figure 12D). Ganglion cells having large rounded euchromatic nucleus but still there are degenerated mitochondria, dilated rough endoplasmic reticulum and cytoplasmic vacuolization. Inner plexiform layer showed some normal nerve axons others are destructed (Figure 13D).

Morphometrical and statistical analysis results

Regarding the total thickness of the rats' retina, there was a highly significant decrease ($P< 0.001$) in group 2 when compared to group 1, a significant decrease ($P< 0.05$) in group 4 when compared to group 1, while group 3 showed non-significance ($P>0.05$) compared to group 1. There was a highly significant increase ($P< 0.001$) in group 3 when compared to group 2, a significant increase ($P< 0.05$) in group 4 when compared to group 2. Group 4 showed a significant decrease ($P< 0.05$) in comparison to group 3 (Table 1, Histogram 1).

Thickness of the outer and inner nuclear layers of the retina, demonstrates a highly significant decrease ($P< 0.001$) in comparing group 2 to group 1, a non-significance ($P>0.05$) when compared group 3 and 4 to group 1 and a highly significant increase ($P< 0.001$) when comparing group 3 and 4 to group 2. With a non-significance ($P>0.05$) between group 3 and 4 (Table 1, Histogram 1).

Regarding the number of the ganglion cells, there was a highly significant decrease ($P< 0.001$) in group 2 compared to group 1, a significant decrease ($P< 0.05$) in group 4 compared to group 1, while group 3 showed non-significance ($P>0.05$) when compared to group 1. There was a highly significant increase ($P< 0.001$) in group 3 compared to group 2, a significant increase ($P< 0.05$) in group 4 when compared to group 2. Group 4 showed a significant decrease ($P< 0.05$) in comparison to group 3 (Table 2, Histogram 2).

All immunohistochemical results including TNF-α, VEGF, vimentin, and caspase-3, illustrated a highly significant increase of positive immunoreaction ($P< 0.001$) in group 2 when compared to group 1, a non-significance ($P>0.05$) when compared group 3 and 4 to group 1. Group 3 and 4 showed a highly significant decrease ($P< 0.001$) in comparison to group 2. With a non-significance ($P>0.05$) between group 3 and 4 (Table 3, Histogram 3).

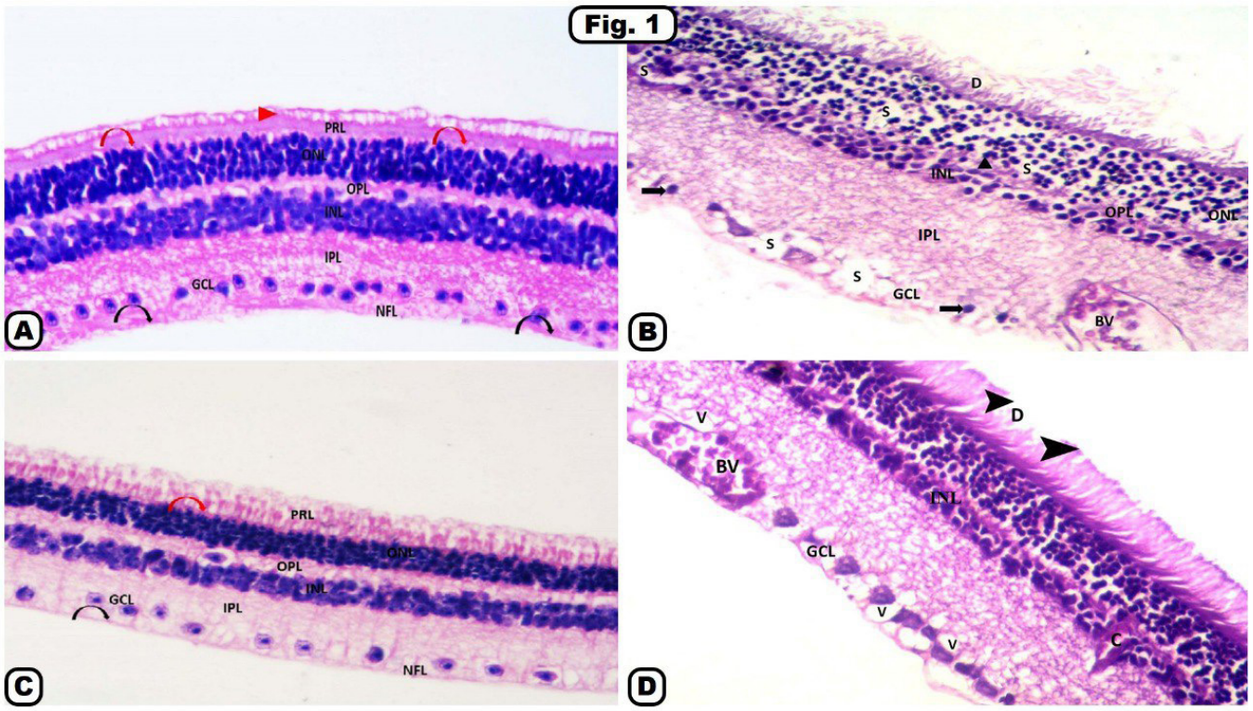

Fig.1: A photomicrograph of a retinal section stained with Hematoxylin and eosin demonstrating:
A: Group 1 (Normal Control): showing normal histological structure of well-organized retinal layers from outside inwards are retinal pigment epithelium (arrow head), photoreceptor layer (PRL), outer limiting membrane (red curved arrow), outer nuclear layer (ONL), outer plexiform layer (OPL), inner nuclear layer (INL), inner plexiform layer (IPL), ganglion cell layer (GCL), and nerve fiber layer (NFL) and inner limiting membrane (black curved arrow).
B: Group 2 (Diabetic Control): showing marked disorganization of retinal layers with appearance of empty spaces (S) between the nuclei of outer nuclear layer (ONL), inner nuclear layer (INL) and ganglion cell layer (GCL). degenerated photoreceptor layer is also detected (D). Outer plexiform layer (OPL) showing disruption (arrow head). ganglion cells appeared with pycnotic nuclei (arrow). Notice, large congested blood vessel (BV) seen within the ganglion cell layer (GCL) extending to IPL.
C: Group 3 (Diabetes+Avocado soybean): showing retinal layers, more or less like control group, formed of photoreceptor layer (PRL), outer limiting membrane (red curved arrow), outer nuclear layer (ONL), outer plexiform layer (OPL), inner nuclear layer (INL), inner plexiform layer (IPL), ganglion cell layer (GCL), nerve fiber layer (NFL) and inner limiting membrane (black curved arrow).
D: Group 4 (Diabetes+Glibenclamide): still showing degenerated retinal pigment epithelium (arrow head) and photoreceptors layer (D), small capillary (C) within inner nuclear layer (INL). ganglion cell layer (GCL) showed vacuolation (V) and congested blood vessel (BV).
(Hematoxylin and eosin, ×200)

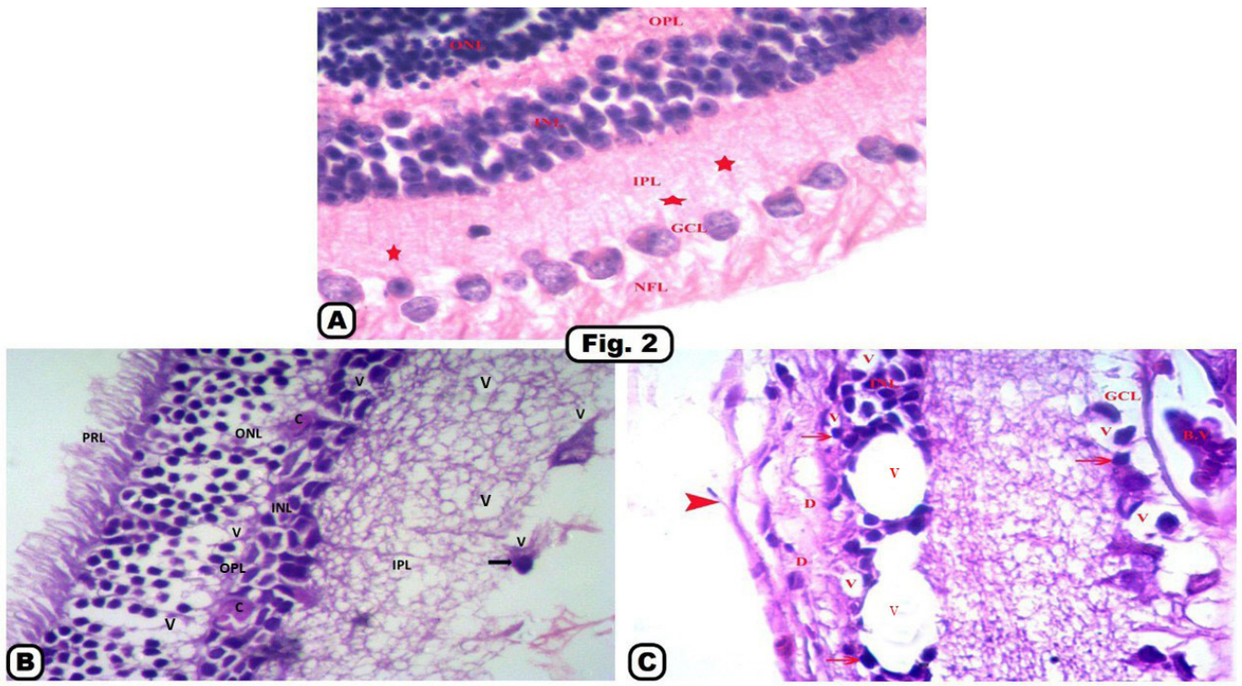

Fig. 2: A photomicrograph of a retinal section stained with Hematoxylin and eosin demonstrating:
A: Group 1 (Normal Control): showing outer nuclear layer (ONL), formed of several rows of the bodies of rods and cones and their densely stained nuclei. Outer plexiform layer (OPL), cells in inner nuclear layer (INL) are larger with paler nuclei than those of the ONL, inner plexiform layer (IPL) has a thick pale eosinophilic fibrillary appearance. Ganglion cell layer (GCL), composed of a single row of ganglion cells displaying abundant light-stained cytoplasm. They have vesicular spherical or angular nuclei with prominent nucleoli, and nerve fiber layer (NFL) contains the processes of ganglion cells. Supporting fibers from Muller's cells (star) are also seen.
B: Group 2 (Diabetic Control): showing degenerated photoreceptor layer (PRL) and multiple vacuolation (V) within outer nuclear layer (ONL), inner nuclear layer (INL) and inner plexiform layer (IPL). Notice, most of ganglion cells were lost, others appeared with pycnotic nuclei (arrow), narrowing of outer plexiform layer (OPL) and small capillaries (C) appeared within inner nuclear layer (INL).
C: Group 2 (Diabetic Control): showing marked disorganization of retinal layers, degenerated retinal pigment epithelium (arrow head), degenerated photoreceptors and outer nuclear layers (D), pycnotic nuclei (arrow) within inner nuclear layer (INL), and ganglion cell layer (GCL). Notice, multiple vacuolation (V) appeared within inner nuclear layer (INL), and ganglion cell layer (GCL), large congested blood vessel (BV) seen at ganglion cell layer (GCL) (Hematoxylin and eosin, ×400)

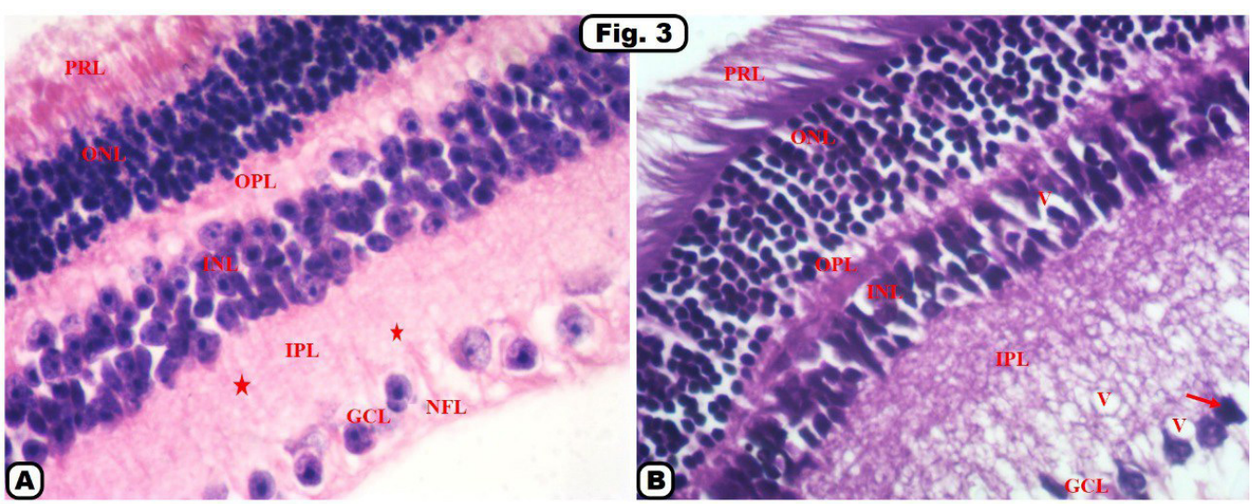

Fig.3: A photomicrograph of a retinal section stained with Hematoxylin and eosin demonstrating:A: Group 3 (Diabetes+Avocado soybean): showing retinal layers, more or less like control group, formed of well-organized, photoreceptor layer (PRL), outer nuclear layer (ONL), outer plexiform layer (OPL), inner nuclear layer (INL), and inner plexiform layer (IPL), ganglion cell layer (GCL), and nerve fiber layer (NFL) that contains the processes of ganglion cells. Notice, the supporting fibers from Muller's cells (star). B: Group 4 (Diabetes+Glibenclamide): showing improvement in some retinal layers including, photoreceptor layer (PRL), outer nuclear layer (ONL), outer plexiform layer (OPL). However, there is vacuolation (V) within inner nuclear layer (INL), inner plexiform layer (IPL), and ganglion cell layer (GCL) that also exhibits pycnotic nuclei (arrow). (Hematoxylin and eosin, ×400)

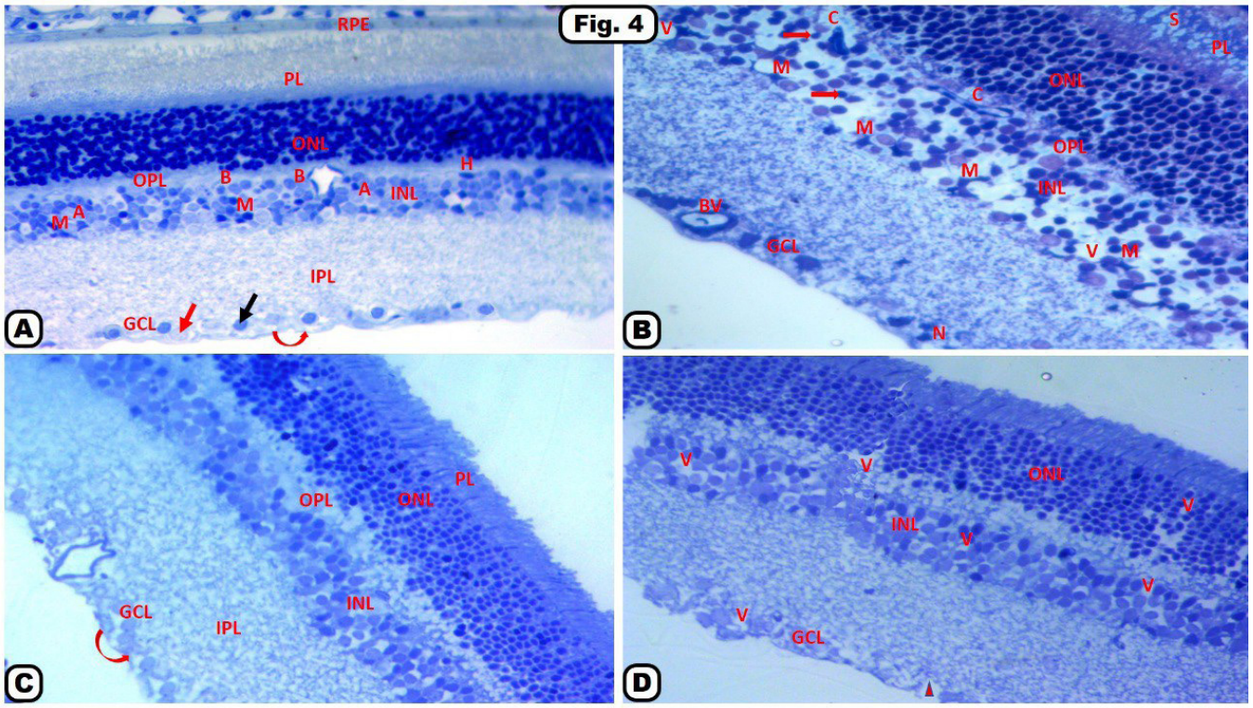

Fig.4: A photomicrograph of a retinal section stained with Toluidine blue demonstrating:
A: Group 1 (Normal Control): showing layers of the retina. Retinal pigment epithelium layer (RPE) cells appear as a single layer of cuboidal cells. The photoreceptor layer (PL) appeared as elongated barrel-shaped structures. The outer nuclear layer (ONL) is formed of several rows of the cell bodies of the rods and cones with their scanty cytoplasm and dark nuclei.
The processes of these cells extend into the outer plexiform layer (OPL). Inner nuclear layer (INL) contains larger cells with paler nuclei than those found in the ONL. Four types of cells could be identified in the INL layer: bipolar cells (B), horizontal cells (H), Muller cells (M), and amacrine cells (A). Inner plexiform layer (IPL) appears thicker than the OPL. Ganglion cell layer (GCL) revealed a single row of light stained cytoplasm and vesicular pale nuclei with prominent nucleoli of ganglion cells (red arrow) and dark stained nuclei of astrocytes (black arrow). Also inner limiting membrane seen as a dark stained line (red curved arrow).
B: Group 2 (Diabetic Control): showing Photoreceptor layer (PL) filled with multiple empty spaces (S). The outer nuclear layer (ONL) appeared with dark stained nuclei, outer plexiform layer (OPL) showed marked thinning. Inner nuclear layer (INL) showed widely separated nuclei (red arrow), cytoplasmic vacuolation (V), many blood capillaries (C), and many Muller cells (M). Ganglion cell layer (GCL) revealed complete degeneration and cytoplasmic lysis of ganglion cells with dissolution of their nuclei (N). Note, the appearance of congested blood vessel (BV) within GCL.
C: Group 3 (Diabetes+Avocado soybean): showing the different retinal layers more or less similar to control group; formed of photoreceptor layer (PL), outer nuclear layer (ONL), outer plexiform layer (OPL), inner nuclear layer (INL), Inner plexiform layer (IPL), Ganglion cell layer (GCL) and inner limiting membrane (red curved arrow).
D: Group 4 (Diabetes+Glibenclamide): showing vacuolation (V) within outer nuclear layer (ONL), inner nuclear layer (INL) and ganglion cell layer (GCL). some ganglion cells are lost (arrow head).
(Toluidine blue, × 200)

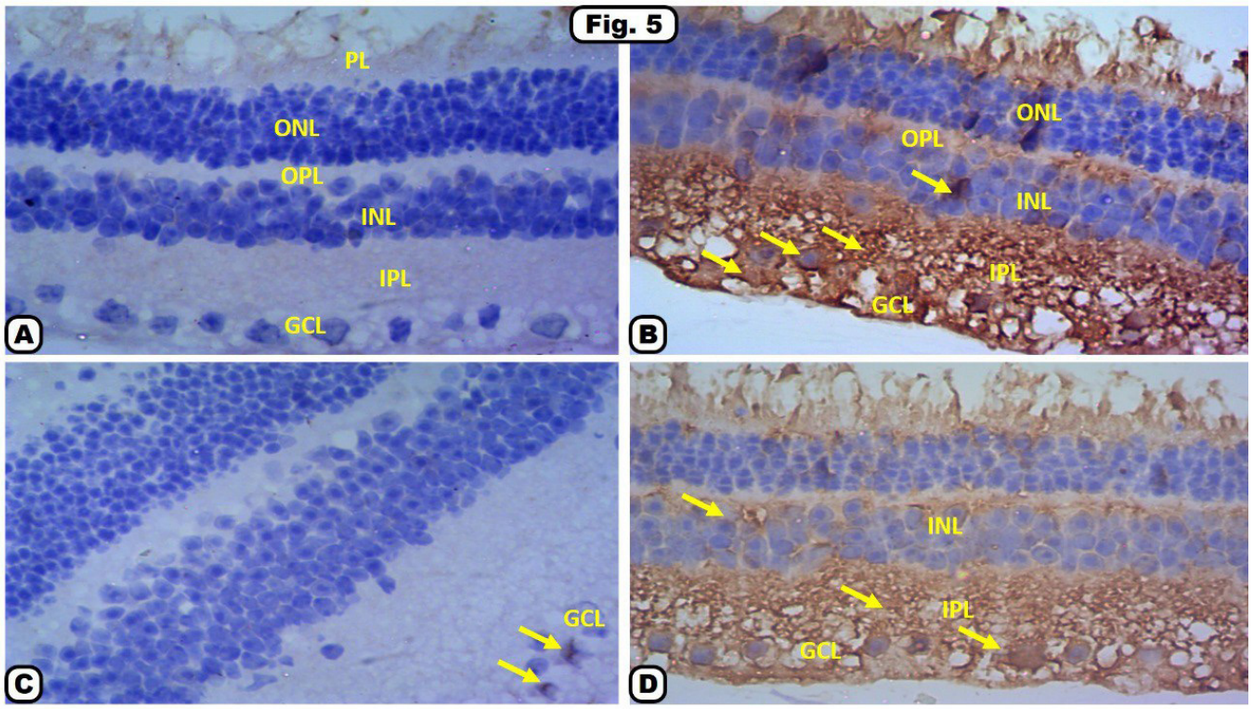

Fig.5: TNF immunohistochemical staining of the retina showing:
A: Group 1 (Normal Control): demonstrating a very weak cytoplasmic intensity in all layers including, photoreceptor layer (PL), outer nuclear layer (ONL), outer plexiform layer (OPL), inner nuclear layer (INL), inner plexiform layer (IPL), and ganglion cell layer (GCL).
B: Group 2 (Diabetic Control): demonstrating a strong positive high intensity immune reaction (arrow) in outer nuclear layer (ONL), outer plexiform layer (OPL), inner nuclear layer (INL), inner plexiform layer (IPL), and ganglion cell layer (GCL).
C: Group 3 (Diabetes+Avocado soybean): demonstrating a weak intensity immune reaction (arrow) appear in ganglion cell layer (GCL).
D: Group 4 (Diabetes+Glibenclamide): demonstrating a moderate intensity immune reaction (arrow) in inner nuclear layer (INL), inner plexiform layer (IPL), and ganglion cell layer (GCL). (TNF x 400 immunostaining)

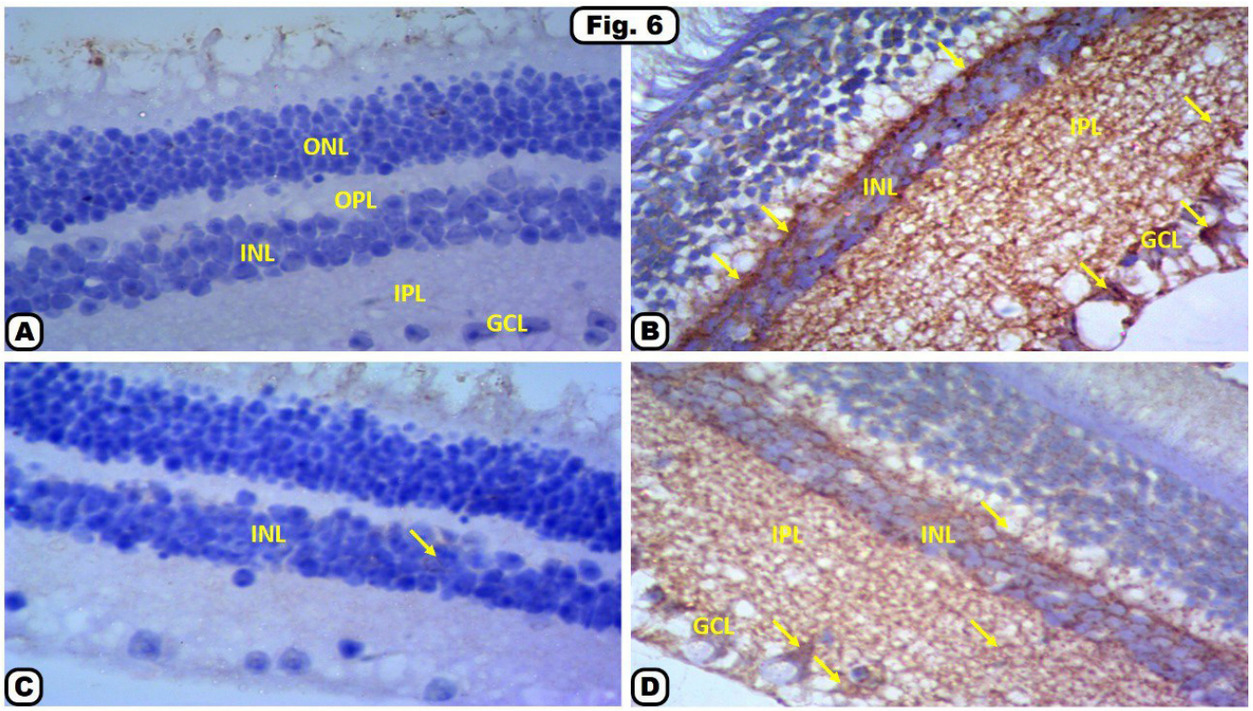

Fig.6: Vascular endothelial growth factor (VEGF) immunohistochemical staining of the retina showing:
A: Group 1 (Normal Control): illustrating a negative immunoreaction in outer nuclear layer (ONL), outer plexiform layer (OPL), inner nuclear layer (INL), inner plexiform layer (IPL), and ganglion cell layer (GCL).
B: Group 2 (Diabetic Control): illustrating a strong positive cytoplasmic immunoreaction intensity (arrow) in inner nuclear layer (INL), inner plexiform layer (IPL), and ganglion cell layer (GCL).
C: Group 3 (Diabetes+Avocado soybean): illustrating a very weak immunoreaction intensity (arrow) in inner nuclear layer (INL).
D: Group 4 (Diabetes+Glibenclamide): illustrating a moderate immunoreaction intensity appears as brown cytoplasmic deposits (arrow) in inner nuclear layer (INL), inner plexiform layer (IPL), and ganglion cell layer (GCL).
(Anti-VEGF immunostaining, ×400).

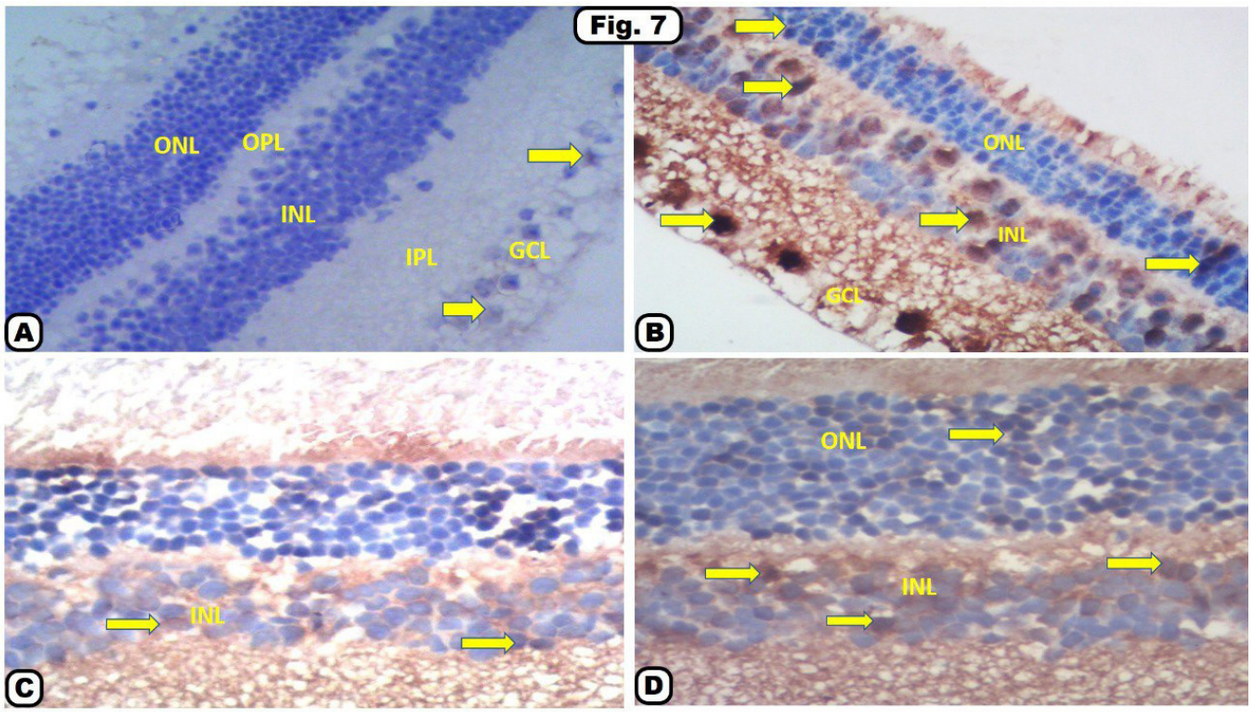

Fig.7: Caspase 3 immunohistochemical staining of the retina showing:
A: Group 1 (Normal Control): demonstrating a very weak cytoplasmic immune reaction intensity for caspase-3 (arrow) in outer nuclear layer (ONL), outer plexiform layer (OPL), inner nuclear layer (INL), inner plexiform layer (IPL), and ganglion cell layer (GCL).
B: Group 2 (Diabetic Control): demonstrating a strong positive high intensity immune reaction for caspase-3 (arrow) in outer nuclear layer (ONL), inner nuclear layer (INL), and ganglion cell layer (GCL).
C: Group 3 (Diabetes+Avocado soybean): showing a weak intensity immune reaction for caspase-3 (arrow) in inner nuclear layer (INL).
D: Group 4 (Diabetes+Glibenclamide): showing a moderate intensity immune reaction for caspase-3 (arrow) in outer nuclear layer (ONL), and inner nuclear layer (INL).
(Caspase-3 x 400 immunostaining)

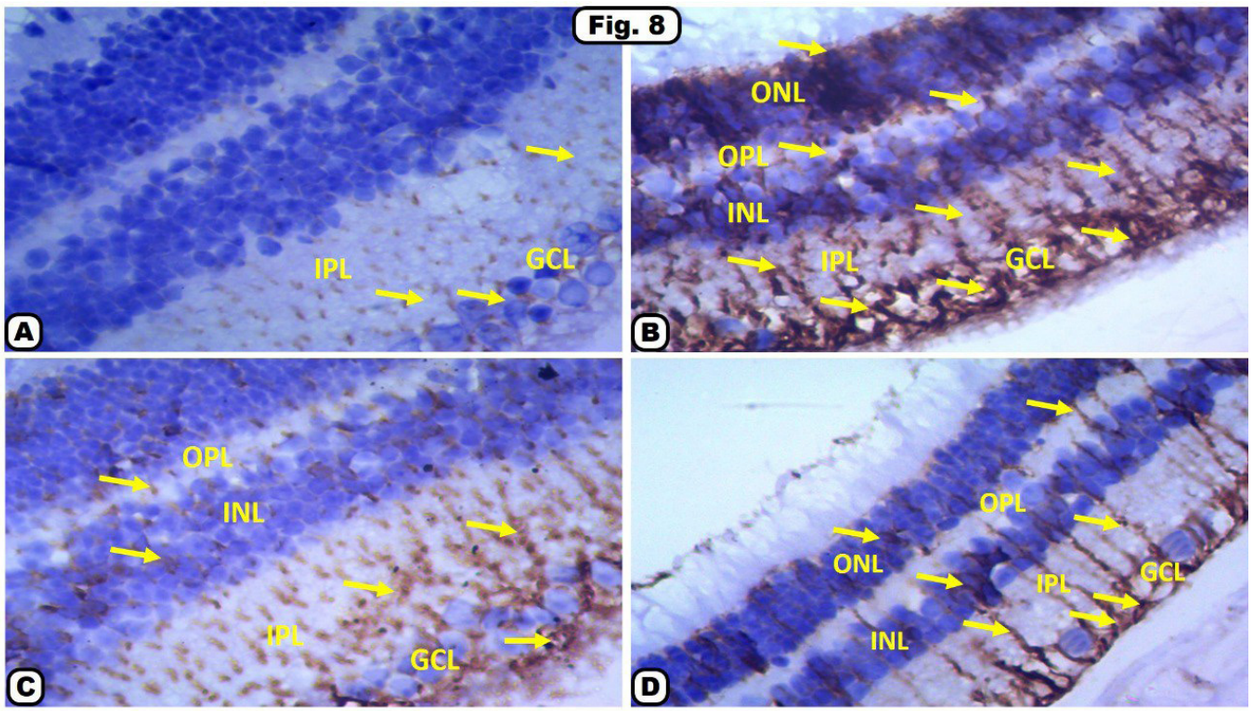

Fig.8: Vimentin immunohistochemical staining of the retina demonstrating:
A: Group 1 (Normal Control): showing a very weak immunoreactivity in the Muller cell end feet and Muller fibers (arrow) found in inner plexiform layer (IPL) and ganglion cell layer (GCL).
B: Group 2 (Diabetic Control): showing a strong positive immunoreactivity in the Muller cell end feet and Muller fibers (arrow) found in outer nuclear layer (ONL), outer plexiform layer (OPL), inner nuclear layer (INL), inner plexiform layer (IPL), and ganglion cell layer (GCL).
C: Group 3 (Diabetes+Avocado soybean): demonstrating a weak immunoreactivity in the Muller cell end feet and Muller fibers (arrow) in outer plexiform layer (OPL), inner nuclear layer (INL), inner plexiform layer (IPL) and ganglion cell layer (GCL).
D: Group 4 (Diabetes+Glibenclamide): demonstrating a moderate immunoreactivity in the Muller cell end feet and Muller fibers (arrow) in outer nuclear layer (ONL), outer plexiform layer (OPL), inner nuclear layer (INL), inner plexiform layer (IPL) and ganglion cell layer (GCL).
(Anti-vimentin immunostaining, ×400)

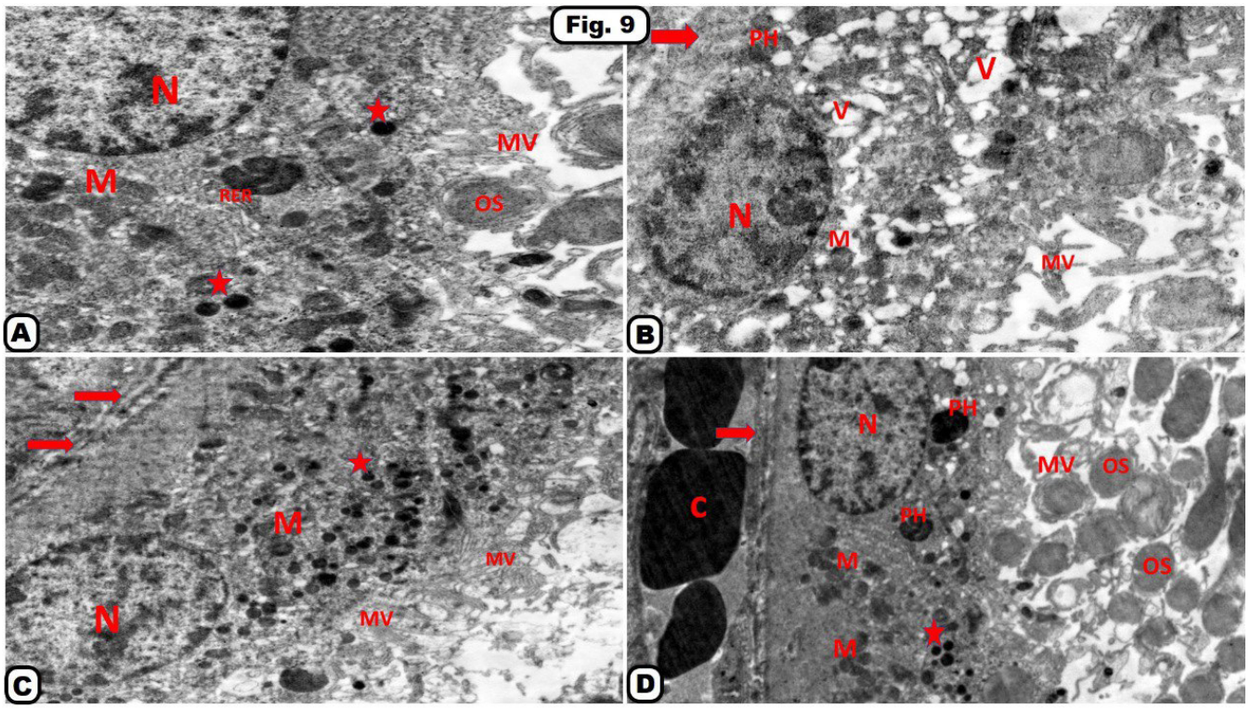

Fig.9: An electron photomicrograph of the rat's retina demonstrating:
A: Group 1 (Normal Control), showing retinal pigment epithelial cell layer having large euchromatic oval nucleus (N), cisterna of rough endoplasmic reticulum (RER), mitochondria (M), melanin granules (star), long apical microvilli (MV) and phagocytosed photoreceptors outer segments (OS).
B: Group 2 (Diabetic Control), showing retinal pigmented cell layer resting on distorted Bruch's membrane (red arrow) with destructed disturbed apical microvilli (MV), small darkly stained nucleus (N) and swollen degenerated mitochondria with destructed cristae (M). There are large phagosomes (PH) and vacuolization (V) in the cytoplasm.
C: Group 3 (Diabetes+Avocado soybean), showing retinal pigment epithelial cell layer resting on nearly normal Bruch's membrane (red arrow), having euchromatic oval nucleus (N), mitochondria (M), melanin granules (star) and long apical microvilli (MV), more or less like control group.
D: Group 4 (Diabetes+Glibenclamide), showing retinal pigment epithelial cell layer, resting on Bruch's membrane (red arrow) separating it from the chorio-capillary layer (C), having euchromatic oval nucleus (N), mitochondria (M), melanin granules (star) and phagocytosed photoreceptors outer segments (OS). But still there are degenerated microvilli (MV), and large phagosomes (PH).
(TEMX3000)

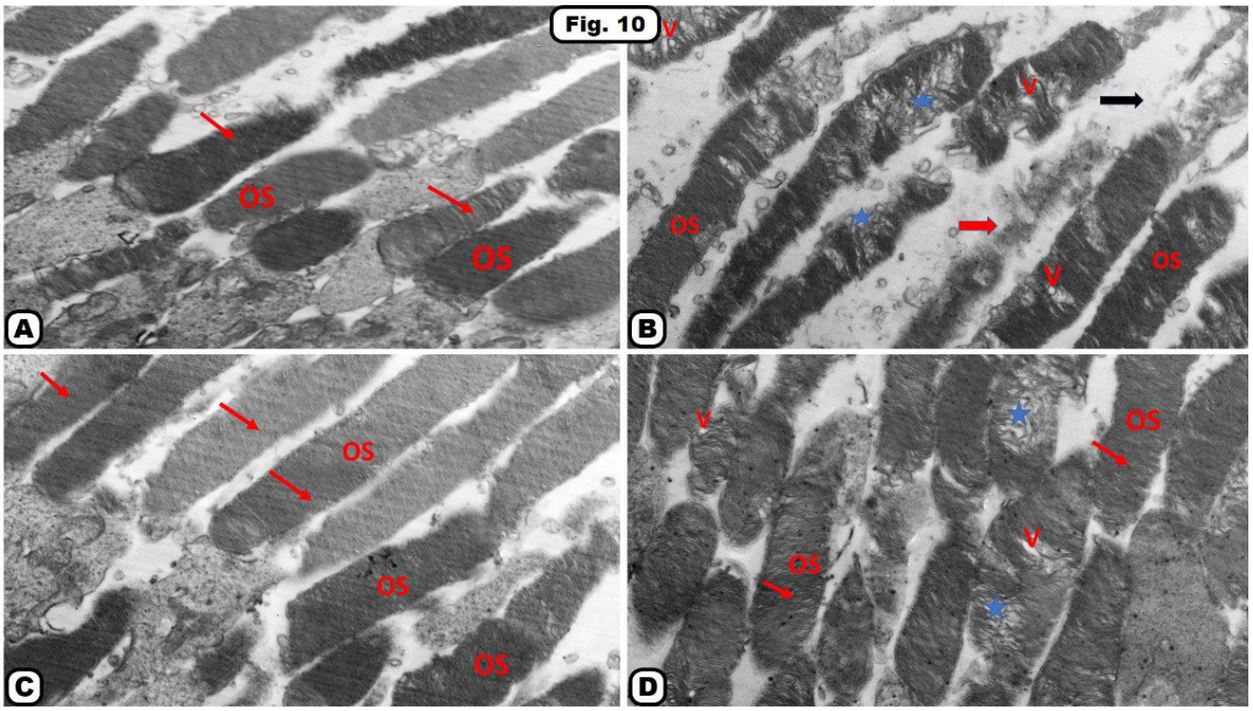

Fig.10: An electron photomicrograph of a section of the rat's retina demonstrating:
A: Group 1 (Normal Control), showing the outer segments photoreceptors (OS) appear as long, straight, and cylindrical structures containing regular flat horizontal lamellar discs (red arrow).
B: Group 2 (Diabetic Control), showing Multiple photoreceptors outer segments (OS) are separated by wide spaces (black arrow). Some of these outer segments are degenerated (red arrow), others showing vacuolation (V) and distorted lamellar discs (blue star).
C: Group 3 (Diabetes+Avocado soybean), showing improved photoreceptors outer segments (OS) with intact regular flattened horizontal lamellar discs (red arrow), more or less like control group.
D: Group 4 (Diabetes+Glibenclamide), showing some improved photoreceptors outer segments (OS) with regular flattened horizontal lamellar discs (red arrow), but some segments still showing vacuolation (V) and distorted lamellar discs (blue star).
(TEMX4000)

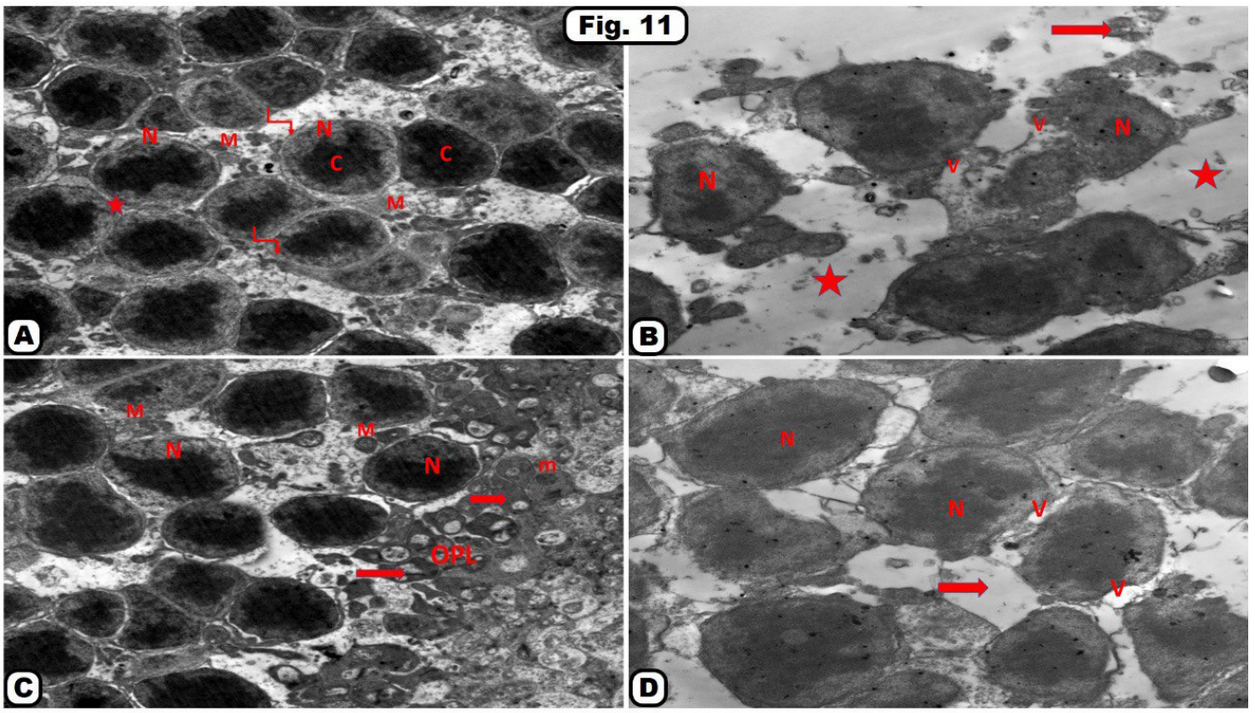

Fig.11: An electron photomicrograph of a section of the rat's retina illustrating:
A: Group 1 (Normal Control), showing the outer nuclear layer with rounded centrally located nuclei (N) with highly condensed heterochromatin (C), surrounded by a thin rim of cytoplasm (angled arrow) and mitochondria (M). Notice the cells are tightly backed with no intercellular spaces (star).
B: Group 2 (Diabetic Control), from the outer nuclear layer showing cells with dark stained nuclei (N), and cells with cytoplasmic vacuolization (V). The nuclei are separated by wide intercellular spaces (star) filled with debris (red arrow).
C: Group 3 (Diabetes+Avocado soybean), showing the outer nuclear layer with rounded centrally located nuclei (N) surrounded by mitochondria (M). Small area of the outer plexiform layer (OPL) can be seen having intact nerve axons (red arrow) and containing mitochondria (m).
D: Group 4 (Diabetes+Glibenclamide), showing the outer nuclear layer with rounded centrally located nuclei (N) but there are cytoplasmic vacuolation (V) and the nuclei are separated by wide intercellular spaces (red arrow).
(TEM, X3000)

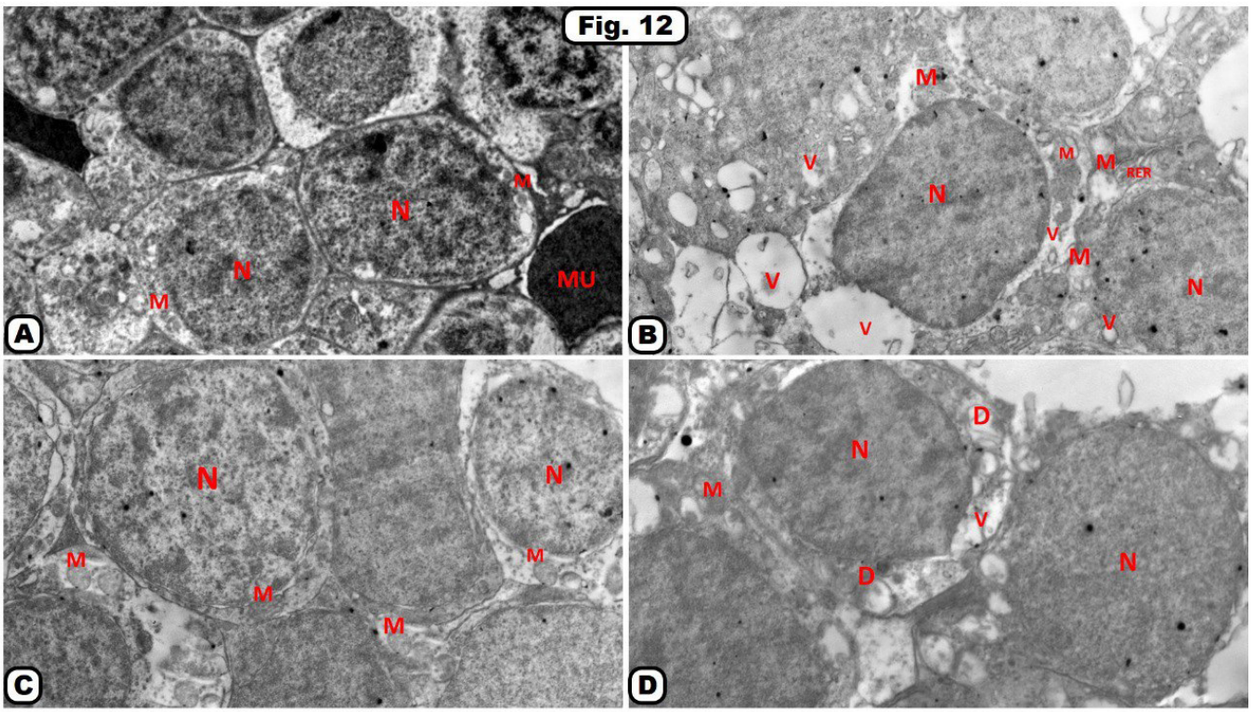

Fig.12: An electron photomicrograph of the rat's retina illustrating:
A: Group 1 (Normal Control), from the inner nuclear layer showing the cell bodies of bipolar cells, tightly packed to each other and having euchromatic rounded nuclei (N), rounded or elliptical in shape and surrounded by thin rim of cytoplasm filled with mitochondria (M). Muller cells contain nuclei of high density (MU).
B: Group 2 (Diabetic Control), showing inner nuclear layer cells having condensed nuclei (N), swollen degenerated mitochondria with distorted cristae (M), many cytoplasmic vacuolization (V), and dilated rough endoplasmic reticulum (RER).
C: Group 3 (Diabetes+Avocado soybean), from the inner nuclear layer showing the cell bodies of bipolar cells, tightly packed to each other and having euchromatic rounded nuclei (N), smooth contour of mitochondria (M) more or less like control.
D: Group 4 (Diabetes+Glibenclamide), from the inner nuclear layer showing bipolar cells with euchromatic rounded nuclei (N), some mitochondria are normal (M) others are degenerated (D). vacuolation of the cytoplasm (V) also seen.
(TEM X3500)

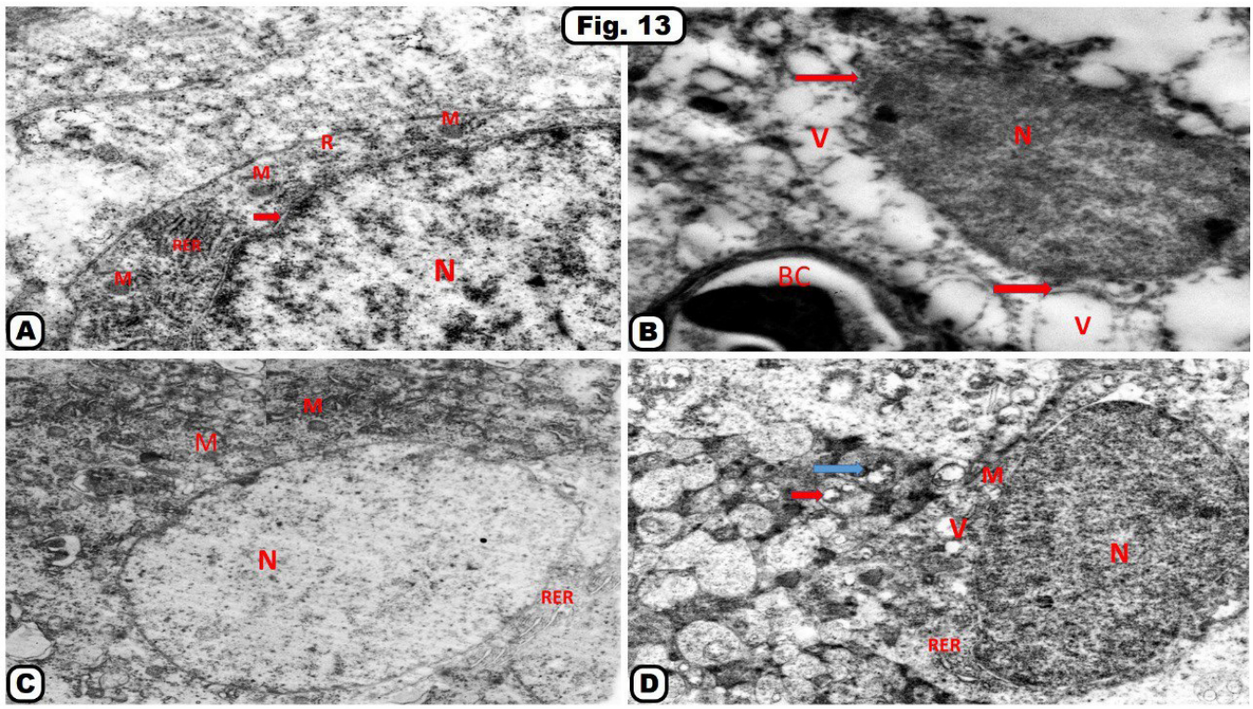

Fig.13: An electron photomicrograph of the rat's retina demonstrating:
A: Group 1 (Normal Control), showing ganglion cell having large rounded euchromatic nucleus (N) with intact nuclear envelope (red arrow) surrounded by thin rim of cytoplasm containing mitochondria (M), rough endoplasmic reticulum (RER) and scattered ribosomes (R) are observed.
B: Group 2 (Diabetic Control), showing ganglion cell with indented irregular nucleus (N), and destructed nuclear membrane (red arrow). The cytoplasm is vacuolated (V). Note congested blood capillary (BC) is seen.
C: Group 3 (Diabetes+Avocado soybean), showing ganglion cell having large rounded nucleus (N) surrounded by thin rim of cytoplasm containing mitochondria (M), Rough endoplasmic reticulum (RER) more or less like control.
D: Group 4 (Diabetes+Glibenclamide), showing ganglion cell having large rounded euchromatic nucleus (N) but still there are degenerated mitochondria (M), dilated rough endoplasmic reticulum (RER) and cytoplasmic vacuolization (V). Notice, inner plexiform layer showing some normal nerve axons (red arrow) others are destructed (blue arrow).
(TEM X4000)

Table 1: Mean ±SD and range of the total thickness of the rats' retina and the thickness of its outer and inner nuclear layers in all groups

	Group 1	Group 2	Group 3	Group 4	U	*P value*
Total retinal thickness					3.79	<0.001[1]
Mean ±SD	123.207.07±	83.106.94±	117.50±7.89	103.7011.79±	1.44	0.15[2]
Range	110 – 129	70 – 95	104 – 127	85 – 119	3.11	0.007[3]
					3.78	<0.001[4]
					3.10	0.003[5]
					2.42	0.02[6]
Outer nuclear thickness					3.78	<0.001[1]
Mean ±SD	40.90±4.53	25.80±3.71	38.20±3.22	37.10±3.41	1.25	0.21[2]
Range	35 – 50	20 – 31	34 – 43	30 – 40	1.64	0.10[3]
					3.78	<0.001[4]
					3.68	<0.001[5]
					0.50	0.62[6]
Inner nuclear thickness					3.79	<0.001[1]
Mean ±SD	26.80±2.70	15.70±٣،53	28.90±2.69	27.903.54±	1.53	0.13[2]
Range	23 – 31	12 – 22	24 – 33	20 – 31	1.11	0.27[3]
					3.78	<0.001[4]
					3.68	<0.001[5]
					0.38	0.70[6]

u = Mann Whitney U test
1 = comparing group 1 & group 2
2 = comparing group 1 & group 3
3 = comparing group 1 & group 4
4 = comparing group 2 & group 3
5 = comparing group 2 & group 4
6 = comparing group 3 & group 4

Table 2: Mean ±SD and range of the number of ganglion cells of the rats' retina in all groups

	Group 1	Group 2	Group 3	Group 4	U	*P value*
Number of ganglion cells					3.79	<0.001[1]
Mean ±SD	8.70±1.50	2.93±1.69	7.35±1.62	5.64±1.36	1.52	0.13[2]
Range	7 – 12	1 – 6.8	4.2 – 10	3.7 – 7.3	2.43	0.01[3]
					3.55	<0.001[4]
					2.98	0.008[5]
					2.46	0.01[6]

u = Mann Whitney U test 1 = comparing group 1 & group 2 2 = comparing group 1 & group 3
3 = comparing group 1 & group 4 4 = comparing group 2 & group 3 5 = comparing group 2 & group 4
6 = comparing group 3 & group 4

Table 3: Mean ±SD and range of the area % of TNF-α, VEGF, vimentin, and caspase-3 positive immunohistochemical reaction in all groups

	Group 1	Group 2	Group 3	Group 4	U	*P value*
TNF-α					3.78	<0.001[1]
Mean ±SD	4.97±2.10	31.91±4.07	5.28±1.77	7.20±3.26	0.19	0.85[2]
Range	0.88 – 7.4	25.2 – 36.7	2.4 – 8.2	3.5 – 13.4	1.40	0.16[3]
					3.78	<0.001[4]
					3.78	<0.001[5]
					1.33	0.19[6]
VEGF					3.78	<0.001[1]
Mean ±SD	4.45±1.56	28.57±4.81	5.36±1.52	6.25±2.37	1.17	0.24[2]
Range	2.5 – 6.5	22.5 – 35.5	3.5 – 8.1	3.5 – 9.3	1.74	0.08[3]
					3.78	<0.001[4]
					3.78	<0.001[5]
					0.76	0.45[6]
Vimentin					3.78	<0.001[1]
Mean ±SD	8.32±1.28	36.18±4.97	9.27±3.91	13.90±6.07	0.53	0.60[2]
Range	6.7 – 10.2	23.5 – 40.8	4.3 – 15.6	6.2 – 22.1	1.70	0.09[3]
					3.78	<0.001[4]
					3.78	<0.001[5]
					1.66	0.10[6]
Caspase intensity					3.78	<0.001[1]
Mean ±SD	15.27±4.22	62.24±5.36	16.58±6.94	19.08±4.45	0.15	0.88[2]
Range	6.5 – 22.3	54 – 68	9.5 – 28.9	13.5 – 28.3	1.74	0.08[3]
					3.78	<0.001[4]
					3.78	<0.001[5]
					1.06	0.29[6]

u = Mann Whitney U test 1 = comparing group 1 & group 2 2 = comparing group 1 & group 3
3 = comparing group 1 & group 4 4 = comparing group 2 & group 3 5 = comparing group 2 & group 4
6 = comparing group 3 & group 4

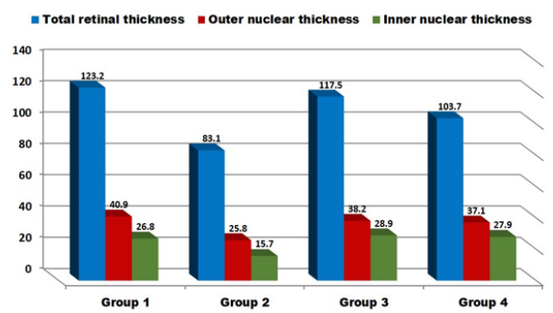

Histogram 1: Mean of the total thickness of the rats' retina and the thickness of its outer and inner nuclear layers in all groups

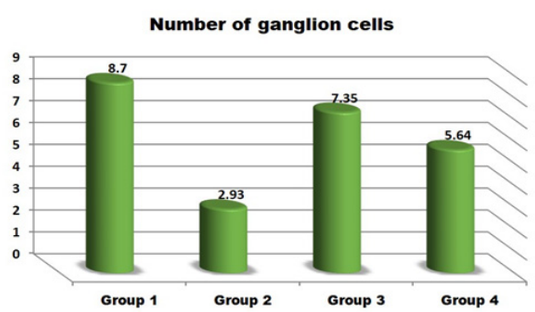

Histogram 2: Mean of the number of ganglion cells of the rats' retina in all groups

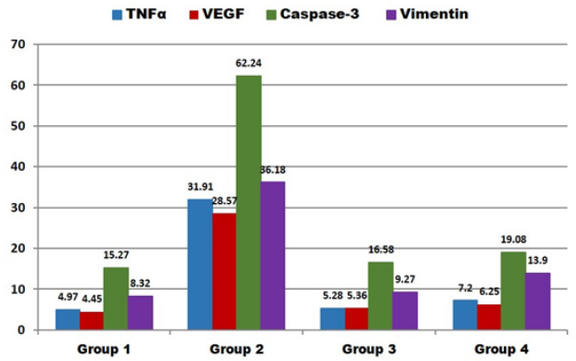

Histogram 3: Mean of the area % of TNF-α, VEGF, vimentin, and caspase-3 positive immunohistochemical reaction in all groups

DISCUSSION

DR is a neurodegenerative, microvascular, and sight-threatening impact of chronic uncontrolled DM[2]. Therefore, conducting researches on prohibition and therapy of DR is of major indication.

In the existing study, we first inspected the curative effects of ASB versus glibenclamide on the DR progression in STZ-induced diabetic rats.

Histological findings of the diabetic rats' retina demonstrated marked disorganization of all the retinal layers, degenerated RPE, PRL, and ONL, with appearance of empty spaces between the nuclei of ONL, INL and GCL. Multiple vacuolation within ONL, INL, IPL, and GCL and cytoplasmic vacuolation in the INL. OPL showing disruption. INL exhibited pycnotic nuclei. These findings coincident with, preceding studies stated that, DR is widely documented by neuronal degeneration that precedes microvascular damage and attributed the loss of cells in DR to neurodegeneration as a result of extended hyperglycemia and microvascular disruption[29,30]. Recent studies strongly confirm the pivotal effect of inflammation in the pathogenesis and development of DR[10,11], where it exhibited characteristics of chronic inflammatory disorders, including increased vascular permeability, inflammatory cell infiltration, and the main expression of pro-inflammatory cytokines and chemokines, which led to edema, tissue damage, and neovascularization in the retina[31,32]. Additionally, elevated expression of vasoactive factors and cytokines may be responsible for structural and functional alterations in the retina[33,34].

Proinflammatory mediator in DR, promoting retinal epithelium damage, as well as accelerating the onset of diabetes[35].

Moreover, in the study GCL revealed total degeneration, lysis of cytoplasm and appearance of pycnotic nuclei with loss of most of the ganglion cells. Together with a highly significant decline in the number of the ganglion cells in comparison to control rats. These findings synchronous with the study that considered the main etiology of DR is the occurrence of mitochondrial dysfunction and damage of ganglion cell of the retina, before occurrence of vascular manifestations[36].

Structural insufficiency of BRB might lead to neuronal cell loss, particularly in the GCL, and also reduces ONL and total retinal thickness[37], similar to the findings, of complete degeneration of GCL with a highly significant decrease of total thickness of the rats' retina and outer and inner nuclear layers of the retina, in the current study.

Retinal ganglion cells degeneration is influenced by many factors, embracing inflammation, oxidative stress, and advanced glycation end products exposure[38,39]. In addition, Daniel *et al*.,[40] observed diabetes-induced loss of RGC and decreased thickness of the retina and stated that these finding, replicated many previous studies that loss of RGC was the prior morphological signs of DR[41,42].

However, others explore no finding of RGC loss, even during chronic diabetes[43]. This conflict may be attributed to different RGC detection methods, quantification, used animals, and the degree of elevated glucose in the studies[44].

Immunohistochemical findings of inflammatory, angiogenesis, and apoptotic makers, TNF-α, VEGF, and caspase-3, in this study revealed a highly significant elevation of positive immunoreaction ($P< 0.001$) compared to the control rats. Concurrent with prior studies, that mitochondria-derived reactive oxygen species induce many DR pathologies including, mitochondrial ROS production, DNA damage, and raised inflammatory mediators and caspase expression, which directly lead to RGC loss[45], and also besides the oxidative stress that aggravates DR, inflammation plays a vital role in the pathogenesis of retinopathy[46,47]. Such elevated levels of oxidative stress and apoptosis in DR have been caused by mitochondrial dysfunction with affection of both retinal neurons and vascular cells by a vicious circle. Where mitochondrial dysfunction invigorates inflammatory mediators and ROS production, that destroys mtDNA, elevates mitochondrial pathology, and progressing to cell death apoptosis[15,48]. Additionally, TNF, IL-1, and IL-6 are mutual proinflammatory cytokines, in vitreous, or retinas of diabetic patients or rats[49].

Moreover, the highly significant increase of positive VEGF immunoreaction in the study, synchronous with many studies proposed that diabetes is a chronic, low-grade inflammatory, and autoimmune disease[49]. Hyperglycemia can prompt leukocyte adhesion to vascular endothelial cells, and this destructing BRB and aggravating microcirculation, leading to retinal hypoxia with increased expression of VEGF. Increased VEGF elevates IL-1β and adhesion factors expression, developing DR[50,51].

Immunohistochemical findings of gliosis maker, vimentin revealed highly significant increase of positive immunoreaction ($P< 0.001$) when compared to the control rats. DR leads to early several degenerative changes as deregulations of glutamate signaling and metabolism,

neural apoptosis, activation of microglial cell and expulsion of pro-inflammatory cytokines; TNF-α[52]. Also, retinal inflammation and elevated ROS in response to DR is the etiology of expression of Müller cells, that excrete cytokines responsible for retinal neuronal and vascular damage[53,54]. Moreover, reactive gliosis in a DR rat model with raised GFAP expression is an indicator of a proinflammatory phenotype[40].

Transmission electron microscopic findings, illustrated destructed disturbed apical microvilli of the retinal pigmented cell layer, small darkly stained nucleus and swollen degenerated mitochondria with destructed cristae. The cytoplasm displayed large phagosomes and vacuolization. Synchronous with, degenerated retinal pigmented epithelium with marked changes in the organelle morphology including; degenerated mitochondria, pyknotic nuclei, and dilated endoplasmic reticulum, in a previous study[55].

Also, in the current study, multiple photoreceptors outer segments are separated by wide spaces. Some of these outer segments are degenerated, others showed vacuolation and distorted lamellar discs, such changes were attributed to the oxidative stress in response to DR[56]. ONL showed cells with dark stained nuclei, others with cytoplasmic vacuolization. The nuclei are separated by wide intercellular spaces with debris. Inner nuclear layer cells having condensed nuclei, swollen degenerated mitochondria with distorted cristae, many cytoplasmic vacuolization, and dilated rough endoplasmic reticulum. In the GCL, ganglion cells appeared with indented irregular nucleus, and destructed nuclear membrane. The cytoplasm is vacuolated, with presence of congested blood capillary, that is also coincident with previous reports that sodium iodate, induced oxidative stress, damaging many retinal organelles[57].

Avocado/soybean composes from avocado fruits, seeds, and soybean oil[58]. Consequently, the mixture of avocado and soybean oil exerts a more potent interactive effects, distinct from action of each component alone[59]. The mixture has acquired a significant role as a natural therapy for numerous diseases[19].

Due to the minimal information on the enormous health benefits of ASB, it was chosen in the current study to provide for the first time, updated information on its benefits on DR induced by STZ versus glibenclamide.

In the current study, Group 3 (Diabetes+Avocado soybean) showed remarkable improvement in inflammatory, apoptotic and gliosis makers demonstrated as a highly significant decrease ($P< 0.001$) compared to group 2 (Diabetic Control) with nearly normal histological appearance and morphometrical analysis that demonstrated a non-significance ($P>0.05$) compared to control.

ASB, has chondro-protective properties, important role in osteoarthritis and autoimmune disorders like rheumatoid arthritis and scleroderma and also has a pivotal anti-inflammatory effects, which are supported by the association of overregulation of pro-inflammatory substrates like interleukins (IL-1β, IL-6, IL-8), macrophage inflammatory proteins, ROS, TNF-α and TNF-β, with autoimmune disorder that is improved by ASB. Also, ASB components of phytosterols, tocopherols, tocotrienols, and isoflavones, has a noticeable reduction on pro-inflammatory substrates in autoimmune and osteoarticular disorders together with remarked structural amelioration in osteoarthritis[19]. Additionally, beneficial effects of ASB related to its avocado oil content that is rich in carotenoids, which can detach cellular O2 performing a protective role against oxidative damage[60]. Moreover, avocado oil improves mitochondrial function in rat's liver under oxidative stress[61]. Adjustment of anti-oxidant enzymes, even in control animals, confirmed that avocado oil has beneficial effects in many metabolic and chronic diseases by diminution of oxidative stress[62].

Glibenclamide, 2nd generation sulphonylureas, has an effective role in medicament of moderate diabetic patients[17].

Histological findings in group 4 (Diabetes+Glibenclamide) showed little improvement than ASB. Where there is still degenerated retinal pigment epithelium and some photoreceptor layer, together with small capillary within inner nuclear layer, vacuolation within INL, IPL, and GCL. Also, there is congested blood vessel, pycnotic nuclei, and lost ganglion cells within ganglion cell layer. Also, immunohistochemical findings of inflammatory, apoptotic and gliosis maker demonstrated a moderate immune reaction intensity. Sulfonylureas, vastly used as hypoglycemic therapy for patients with DM type 2, have neuroprotective effects, synchronous with the improvement in the current study[63]. In diabetic retinal injury, Gli, conserve's retinal structure and function via various models including the transcriptional regulation of antioxidant and neuroprotective genes, and also, has beneficial effects on various DR signs in the goto-kakizaki rats, by limiting diabetes-induced neuro-retinal thickening and the progression of ischemic areas[63]. Moreover, Gli has a protective effect against lipid peroxidation, and oxidative damage in diabetes[22].

Gli repairs by connecting to and prohibiting the ATP-sensitive potassium channels inhibitory sulfonylurea receptor 1 in β-cells of pancreas. This prohibition induces the cell membrane to depolarize, allowing voltage-dependent calcium channels to open. Elevating intracellular calcium in the β-cells with insulin release[64].

Such a slight improvement in histological and immunohistochemical results of Gli compared to ASB. In addition to, the morphometric analysis of the total thickness of the rats' retina, and the number of the ganglion cells in group 4 that still showed a significant decrease ($P< 0.05$) compared to group 3. Results concluded that ASB has the most potent retinal efficacy in DR than glibenclamide.

CONCLUSION

Our hypothesis indicates that diabetes induced structural changes, inflammation, apoptosis, and gliosis in the retina. Avocado/soybean supplementation promotes, potent structure-modifying effects on the diabetic rats' retina induced by STZ via its retinal-protective, anti-inflammatory, anti-oxidative and anti-apoptotic effects, which is more evident than glibenclamide

CONFLICT OF INTERESTS

There are no conflicts of interest.

REFERENCES

1. Standring S: Gray's anatomy the anatomical basis of clinical practice.: Elsevier, London. (2008); 41th ed.: 688–697.
2. Quiroz J, and Yazdanyar A: Animal models of diabetic retinopathy. Ann Transl Med. (2021); 9(15): 1272. doi: 10.21037/atm-20-6737.
3. Wang SY, Andrews CA, Herman WH, Gardner TW, and Stein JD: Incidence and risk factors for developing diabetic retinopathy among youths with type 1 or type 2 diabetes throughout the United States. Ophthalmology. (2017); 124(4): 424-430. doi: 10.1016/j.ophtha.2016.10.031.
4. Antonetti DA, Barber AJ, Bronson SK, Freeman WM, Gardnder TW, Jefferson LS, Kester M, Kimball SR, Krady JK, LaNoue KF, Norbury CC, Quinn PG, Sandirasegarane L, and Simpson LA: Diabetic retinopathy: seeing beyond glucose-induced microvascular disease. Diabetes. (2006); 55(9): 2401-2411. doi: 10.2337/db05-1635.
5. Ahmed N: Advanced glycation endproducts–role in pathology of diabetic complications. Diabetes Res Clin Pract. (2005); 67(1): 3-21. doi: 10.1016/j.diabres.2004.09.004.
6. Curtis TM, Gardiner TA, and Stitt AW: Microvascular lesions of diabetic retinopathy: clues towards understanding pathogenesis? Eye (Lond). (2009); 23(7) 1496-1508. doi: 10.1038/eye.2009.108.
7. Cheung N, Mitchell P, and Wong TY: Diabetic retinopathy. Lancet. (2010); 376(9735): 124-136. doi: 10.1016/S0140-6736(09)62124-3.
8. Nentwich MM, and Ulbig MW: Diabetic retinopathy-ocular complications of diabetes mellitus. World J Diabetes Baishideng Publishing Group Inc. (2015); 6(3): 489-499. doi: 10.4239/wjd.v6.i3.489.
9. Santiago AR, Gaspar JM, Baptista FI, Cristóvão AJ, Santos PF, Kamphuis W, and Ambrósio AF: Diabetes changes the levels of ionotropic glutamate receptors in the rat retina. Mol Vis. (2009); 15: 1620-1630. [PMID: 19693289].
10. Liu X, Ye F, and Xiong H: IL-1β induces IL-6 production in retinal Muller cells predominantly through the activation of p38 MAPK/NF-kappaB signaling pathway. Experimental Cell Research. (2015); 331(1): 223-231. doi: 10.1016/j.yexcr.2014.08.040.
11. Yao Y, Du J, Li R, Zhao L, Luo N, Zhai JY, and Long L: Association between ICAM-1 level and diabetic retinopathy: a review and meta-analysis. Postgrad Med J. (2019); 95(1121): 162-168. doi: 10.1136/postgradmedj-2018-136102.
12. Reddy MA, Zhang E, and Natarajan R: Epigenetic mechanisms in diabetic complications and metabolic memory. Diabetologia. (2015); 58(3): 443-455. doi: 10.1007/s00125-014-3462-y.
13. Stitt AW, Curtis TM, Chen M, Medina RJ, McKay GJ, Jenkins A, Gardiner TA, Lyons TJ, Hammes H, Simó R, and Lois N: The progress in understanding and treatment of diabetic retinopathy. Prog Retin Eye Res. (2016); 51: 156-186. doi: 10.1016/j.preteyeres.2015.08.001.
14. Bandello F, Toni D, Porta M, and Varano M: Diabetic retinopathy, diabetic macular edema, and cardiovascular risk: The importance of a long-term perspective and a multidisciplinary approach to optimal intravitreal therapy. Acta Diabetol. (2020); 57(5): 513-526. doi: 10.1007/s00592-019-01453-z.
15. Bonfiglio V, Platania CBM, Lazzara F, Conti F, Pizzo C, Reibaldi M, Russo A, Fallico M, Ortisi E, Pignatelli F, Longo A, Avitabile T, Drago F, and Bucolo C: TGF-β Serum Levels in Diabetic Retinopathy Patients and the Role of Anti-VEGF Therapy. Int J Mol Sci. (2020); 21(24): 9558. doi: 10.3390/ijms21249558.
16. Wang W, and Lo ACY: Diabetic Retinopathy: Pathophysiology and Treatments. Int J Mol Sci. (2018); 19(6): 1816. doi: 10.3390/ijms19061816.
17. Ebrahimi B, Forouzanfar F, Azizi H, Sarkarizi HK, Sadeghnia H, and Rajabzadeh A: Effect of Electroacupuncture and Glibenclamide on Blood Glucose Level and Oxidative Stress Parameters in Streptozotocin-Induced Diabetic Rats and Possible Human Implications. Acupuncture & Electro-Therapeutics Research. (2020); 44(3): 213-228. doi:10.3727/036012920X15779969212955.
18. Rouhi-Boroujeni H, Rouhi-Boroujeni H, Gharipour M, Mohammadizadeh F, Ahmadi S, and Rafieian-Kopaei M: Systematic review on safety and drug interaction of herbal therapy in hyperlipidemia: a guide for internist. Acta Biomed. (2015); 86(2):130-6. [PMID: 26422426].
19. Salehi B, Rescigno A, Dettori T, Calina D, Docea AO, Singh L, Cebeci F, Özçelik B, Bhia M, Beirami AD, Sharifi-Rad J, Sharopov F, Cho WC, and Natália Martins N: Avocado-Soybean Unsaponifiables: A Panoply of Potentialities to Be Exploited. Biomolecules. (2020); 10(1): E130. doi: 10.3390/biom10010130.

20. Au RY, Al-Talib TK, Au AY, Phan PV, and Frondoza CG: Avocado soybean unsaponifiables (ASU) suppress TNF-α, IL-1β, COX-2, iNOS gene expression, and prostaglandin E2 and nitric oxide production in articular chondrocytes and monocyte/macrophages. Osteoarthritis Cartilage. (2007); 15(11): 1249-1255. doi: 10.1016/j.joca.2007.07.009.
21. Reagan-Shaw S, Nihal M, and Ahmad N: Dose translation from animal to human studies revisited. FASEB J. (2008); 22(3): 659-61. doi: 10.1096/fj.07-9574LSF.
22. Obi BC, Okoye TC, Okpashi VE, Igwe CN, and Alumanah EO: Comparative Study of the Antioxidant Effects of Metformin, Glibenclamide, and Repaglinide in Alloxan-Induced Diabetic Rats. J Diabetes Res. (2016); 2016: 1635361. doi: 10.1155/2016/1635361.
23. Zhang X, Peng L, Dai Y, Sheng X, Chen S, and Xie Q: Effects of Coconut Water on Retina in Diabetic Rats. Evid Based Complement Alternat Med. (2020); 2020: 9450634. doi.org/10.1155/2020/9450634.
24. Nakatsu N, Igarashi Y, Aoshi T, Hamaguchi I, Saito M, Mizukami T, Momose H, Ishii KJ, and Yamada H. Isoflurane is a suitable alternative to the ether for anesthetizing rats before euthanasia for gene expression analysis. J Toxicol Sci. 2017; 42(4):491-497. doi: 10.2131/jts.42.491.
25. Suvarna SK, Layton C, and Bancroft JD: Bancroft's Theory and Practice of Histological Technique. Elsevier, (2013); 7th ed.: 173-214.
26. Suvarna SK, Layton C, and Bancroft JD: Bancroft's Theory and Practice of Histological Techniques. Elsevier, (2019); 8th ed.: 19: 337-394.
27. Jackson P, Blythe D, Bancroft JD, and Gample M: Immunohistochemical techniques in theory and practice of histological technique. Elsevier, China. (2008); 6th ed.: 423.
28. Bozzola JJ: Conventional specimen preparation techniques for transmission electron microscopy of cultured cells. Methods Mol Biol. (2007); 1117: 1-19. doi: 10.1007/978-1-59745-294-6_1.
29. Duh EJ, Sun JK, and Stitt AW: Diabetic retinopathy: Current understanding, mechanisms, and treatment strategies. JCI Insight. (2017); 2(14): e93751. doi: 10.1172/jci.insight.93751.
30. Lim HB, Shin YI, Lee MW, Koo H, Lee WH, and Kim JY: Ganglion Cell - Inner Plexiform Layer Damage in Diabetic Patients: 3-Year Prospective, Longitudinal, Observational Study. Sci Rep. (2020); 10(1): 1470. doi: 10.1038/s41598-020-58465-x.
31. Liou GI: Diabetic retinopathy: Role of inflammation and potential therapies for anti-inflammation. World J. Diabetes. (2010); 1(1): 12-18. doi: 10.4239/wjd.v1.i1.12.
32. Tang J, and Kern TS: Inflammation in diabetic retinopathy. Prog. Retin. Eye Res. (2011); 30(5): 343-58. doi: 10.1016/j.preteyeres.2011.05.002.
33. Khan ZA, and Chakrabarti S: Cellular signaling and potential new treatment targets in diabetic retinopathy. Exp. Diabetes Res. (2007); 2007: 31867. doi: 10.1155/2007/31867.
34. Wirostko B, Wong TY, and Sim ó R: Vascular endothelial growth factor and diabetic complications. Prog Retin Eye Res. (2008); 27(6): 608-21. doi: 10.1016/j.preteyeres.2008.09.002.
35. Gonçalves A, Marques C, Leal E, Ribeiro CF, Reis F, Ambrósio AF, and Fernandes R: Dipeptidyl peptidase- IV inhibition prevents blood-retinal barrier breakdown, inflammation and neuronal cell death in the retina of type 1 diabetic rats. Biochim Biophys Acta. (2014); 1842(9): 1454-1463. doi: 10.1016/j.bbadis.2014.04.013.
36. Alam NM, Mills WC, Wong AA, Douglas RM, Szeto HH, and Prusky GT: A mitochondrial therapeutic reverses visual decline in mouse models of diabetes. Dis Model Mech. (2015); 8(7): 701-710. doi: 10.1242/dmm.020248.
37. Dijk HW, Verbraak FD, Stehouwer M, Kok PH, Garvin MK, Sonka M, DeVries JH, Schlingemann RO, and Abràmoff MD: Association of visual function and ganglion cell layer thickness in patients with diabetes mellitus type 1 and no or minimal diabetic retinopathy. Vision Res. (2011); 51(2): 224-228. doi: 10.1016/j.visres.2010.08.024.
38. Kern TS, and Barber AJ: Retinal ganglion cells in diabetes. J Physiol. (2008); 586(18): 4401–8. doi: 10.1113/jphysiol.2008.156695.
39. Ramadan G A: Sorbitol induced diabetic-like retinal lesions in rats: microscopic study. American Journal of Pharmacology and Toxicology. (2007); 2(2): 89-97. doi:10.3844/ajptsp.2007.89.97.
40. Daniel A, Premilovac D, Foa L, Feng Z, Shah K, Zhang Q, Woolley KL, Bye N, Smith JA, and Gueven N: Novel Short-Chain Quinones to Treat Vision Loss in a Rat Model of Diabetic Retinopathy. Int J Mol Sci. (2021); 22(3): 1016. doi: 10.3390/ijms22031016.
41. Vujosevic S, Muraca A, Alkabes M, Villani E, Cavarzeran F, Rossetti L, and De Cilla S: Early microvascular and neural changes in patients with type 1 and type 2 diabetes mellitus without clinical signs of diabetic retinopathy. Retina. (2019); 39(3): 435-445. doi: 10.1097/IAE.0000000000001990.
42. Platania CBM, Maisto R, Trotta MC, D'Amico M, Rossi S, Gesualdo C, D'Amico G, Balta C, Herman H, Hermenean A, Ferraraccio F, Panarese I, Drago F, and Bucolo C: Retinal and circulating miRNA expression patterns in diabetic retinopathy: An in silico and in *vivo* approach. Br J Pharmacol. (2019); 176(13): 2179-2194. doi: 10.1111/bph.14665.

43. Zheng L, Du Y, Miller C, Gubitosi-Klug RA, Kern TS, Ball S, and Berkowitz BA: Critical role of inducible nitric oxide synthase in degeneration of retinal capillaries in mice with streptozotocin-induced diabetes. Diabetologia. (2007); 50(9): 1987-1996. doi: 10.1007/s00125-007-0734-9.

44. Hajdú RI, Laurik LK, Szabó K, Dékány B, Almási Z, Énzsöly A, Szabó A, Radovits T, Mátyás C, Oláh A, Szél Á , Somfai GM, Dávid C, and Lukáts Á: Detailed Evaluation of Possible Ganglion Cell Loss in the Retina of Zucker Diabetic Fatty (ZDF) Rats. Sci. Rep(2019);9(1):10463. doi: 10.1038/s41598-019-46879-1.

45. Kowluru RA: Diabetic Retinopathy: Mitochondrial Dysfunction and Retinal Capillary Cell Death. Antioxid Redox Signal. (2005); 7(11-12): 1581-87. doi: 10.1089/ars.2005.7.1581.

46. Alviano DS, Rodrigues KF, Leitão SG, Rodrigues ML, Matheus ME, Fernandes PD, Antoniolli AR, and Alviano CS: Antinociceptive and Free Radical Scavenging Activities of Cocos nucifera L. (Palmae) Husk Fiber Aqueous Extract. J Ethnopharmacol. (2004); 92(2-3): 269-273. doi: 10.1016/j.jep.2004.03.013.

47. Sasongko MB, Wong TY, Jenkins AJ, Nguyen TT, Shaw JE, and Wang JJ: Circulating markers of inflammation and endothelial function, and their relationship to diabetic retinopathy. Diabet Med. (2015); 32(5): 686-691. doi: 10.1111/dme.12640.

48. Gueven N, Nadikudi M, Daniel A, and Chhetri J: Targeting mitochondrial function to treat optic neuropathy. Mitochondrion. (2017); 36: 7-14. doi: 10.1016/j.mito.2016.07.013.

49. Mao C, and Yan H: Roles of elevated intravitreal IL-1beta and IL-10 levels in proliferative diabetic retinopathy. Indian J Ophthalmol. (2014); 62(6): 699-701. doi: 10.4103/0301-4738.136220.

50. Capitão M, and Soares R: Angiogenesis and Inflammation Crosstalk in Diabetic Retinopathy. J Cell Biochem. (2016); 117(11): 2443-53. doi: 10.1002/jcb.25575.

51. Fearnley GW, Odell AF, Latham AM, Mughal NA, Bruns AF, Burgoyne NJ, Homer-Vanniasinkam S, Zachary IC, Hollstein MC, Wheatcroft SB, and Ponnambalam S: VEGF-A isoforms differentially regulate ATF-2-dependent VCAM-1 gene expression and endothelial-leukocyte interactions. Mol Biol Cell. (2014); 25(16): 2509-2521. doi: 10.1091/mbc.E14-05-0962.

52. Santiago AR, Gaspar JM, Baptista FI, Cristóvão AJ, Santos PF, Kamphuis W, and Ambrósio AF: Diabetes changes the levels of ionotropic glutamate receptors in the rat retina. Mol Vis. (2009); 15: 1620-1630. [PMID: 19693289].

53. De Hoz R, Rojas B, Ramírez AI, Salazar JJ, Gallego BI, Triviño A, and Ramírez JM: Retinal Macroglial Responses in Health and Disease. Biomed Res Int. (2016), 2016(2954721): 13p. doi. org/10.1155/2016/2954721.

54. Pearsall EA, Cheng R, Matsuzaki S, Zhou K, Ding L, Ahn B, Kinter M, Humphries KM, Quiambao AB, Farjo RA, and Ma JX: Neuroprotective effects of PPARα in retinopathy of type 1 diabetes. PLoS One. (2019); 14(2): 1-17. doi: 10.1371/journal.pone.0208399.

55. Xia T, and Rizzolo LJ: Effects of diabetic retinopathy on the barrier functions of the retinal pigment epithelium. Vision Res. (2017); 139: 72-81. doi: 10.1016/j.visres.2017.02.006.

56. Mohamed MEI, El-Shaarawy EAA, Youakim MF, Shuaib DMA, and Ahmed MM: Aging changes in the retina of male albino rat: a histological, ultrastructural and immunohistochemical study. Folia Morphol (Warsz). (2019); 78(2): 237-258. doi: 10.5603/FM.a2018.0075.

57. Gawish MF, Mazen NF, Hassen EZ, and Adbelhady ME: Light and Electron Microscopic Study on the Possible Ameliorative Role of Adipose-Derived Mesenchymal Stem Cells on Diabetic Retinopathy in Adult Male Albino Rats. EJH. (2018); 41(4): 582-596. DOI: 10.21608/ejh.2018.4129.1011.

58. Maheu E, Cadet C, Marty M, Moyse D, Kerloch I, Coste P, Dougados M, Mazieres B, Spector T, Halhol H, Grouin J, and Lequesne M: Randomised, controlled trial of avocado-soybean unsaponifiable (Piascledine) effect on structure modification in hip osteoarthritis: The ERADIAS study. Ann Rheum Dis. (2014); 73(2): 376-384. doi: 10.1136/annrheumdis-2012-202485.

59. Taylor JF, Goudarzi R, Yazdi PG, and Pedersen BA: In *vitro* effects of arthrocen, an avocado/soy unsaponifiables agent, on inflammation and global gene expression in human monocytes. Int J Chem. (2017); 9(4): 31-39. doi: 10.5539/ijc.v9n4p31.

60. Jang H, Han S, Kim J, Oh S, Jang H, and Kim D: Lactobacillus sakei alleviates high-fat-diet-induced obesity and anxiety in mice by inducing AMPK activation and SIRT1 expression and inhibiting gut microbiota-mediated NF-κB activation. Mol. Nutr. Food Res. (2019); 63(6): e1800978. doi: 10.1002/mnfr.201800978.

61. Han RM, Zhang JP, and Skibsted LH: Reaction Dynamics of Flavonoids and Carotenoids as Antioxidants. Molecules. (2012); 17(2): 2140-2160. doi: 10.3390/molecules17022140.

62. Marques SO, Muller AP, Luciano TF, Tramontin NS, Caetano MS, Pieri BLS, Amorim TL, Oliveira MAL, and Souza CT: Effects of Avocado Oil Supplementation on Insulin Sensitivity, Cognition, and Inflammatory and Oxidative Stress Markers in Different Tissues of Diet-Induced Obese Mice. Nutrients. (2022); 14(14): 2906. doi: 10.3390/nu14142906.

63. Berdugo M, Delaunay K, Lebon C, Naud M, Radet L, Zennaro L, Picard E, Daruich A, Beltrand J, Kermorvant-Duchemin E, Polak M, Crisanti P, and Behar-Cohen FF: Long-Term Oral Treatment with Non-Hypoglycemic Dose of Glibenclamide Reduces Diabetic Retinopathy Damage in the Goto-KakizakiRat Model. Pharmaceutics. (2021); 13(7): 1095. doi.org/10.3390/pharmaceutics13071095.

64. Serrano-Martín X, Payares G, and Mendoza-León A: Glibenclamide, a blocker of K+(ATP) channels, shows antileishmanial activity in experimental murine cutaneous leishmaniasis. Antimicrob Agents Chemother. (2006); 50(12): 4214-6. doi: 10.1128/AAC.00617-06.

الملخص العربى

التأثير الوقائي على شبكية العين للأفوكادو فول الصويا (ASB) مقابل الجليبنكلاميد فى الجرذان المستحثه بداء السكرى الناجم عن الستربتوزوتوسين

رشا ممدوح سلامة[١]، سهام أحمد محمد عبد العزيز[٢]

[١]قسم التشريح والأجنة، [٢]قسم الهستولوجي وبيولوجيا الخلية، كلية الطب، جامعة المنوفي ، مصر

المقدمة: اعتلال الشبكية السكري هو التنكس العصبي و تأثير الأوعية الدموية الدقيقة والتهديد البصرى لمرض السكري المزمن غير المنضبط. لقد اكتسب الأفوكادو فول الصويا، وهو مزيج غذائي جديد نسبيًا، دورًا مهمًا كعلاج طبيعي بديل للعديد من الأمراض. الجليبنكلاميد، وهو سلفونيل يوريا قوي، تم تأكيده في الولايات المتحدة كعلاج لمرض السكري.
الهدف من البحث: استكشاف التأثيرات الوقائية للأفوكادو فول الصويا مقابل الجليبنكلاميد على شبكية الجرذان المصابة بداء السكري التي يسببها الستربتوزوتوسين.
المواد والطرق: تم تصنيف أربعين جرذا إلى أربع مجموعات: المجموعة الضابطة، مجموعة مرض السكري، مجموعة مرض السكري + الأفوكادو فول الصويا، مجموعة مرض السكري + الجليبنكلاميد. تمت معالجة عينات الشبكية من أجل الدراسات النسيجية والهستوكيميائية المناعية والمجهرالإلكترونى. كما تم إجراء دراسات مورفومترية وإحصائية.
النتائج: أظهرت عينة الشبكية للجرذان المصابة بمرض السكرى عدم تنظيم واضح لطبقات الشبكية، وتلف فى طبقة الخلايا الطلائية الملونة، والمستقبلات الضوئية، والطبقة النووية الخارجية مع ظهور فراغات وفجوات متعددة. معظم الخلايا العقدية فقدت، وظهرالبعض الآخرمع نوى متجمعة .بالإضافة إلى انخفاض ملحوظ في السماكة الكلية، وسماكة الطبقات النووية الخارجية والداخلية لشبكية الفئران، وعدد الخلايا العقدية. أوضح التعبير المناعي لـ TNF-α،VEGF caspase،-٣ ، vimentin إرتفاعًا ملحوظا.
نتائج البنية التحتية لطبقة الخلايا الطلائية الملونة في شبكية العين أظهرت تورم وتحلل الميتوكوندريا مع فجوة بالسيتوبلازم. وأظهرت تحلل المستقبلات الضوئية مع فجوات. كما تحتوي الخلايا العقدية على نواة مسننة غير منتظمة وتدمير فى الغشاء النووي وفجوة بالسيتوبلازم. يعدل الأفوكادو فول الصويا تغيرات اعتلال الشبكية السكري، بنائيا وهستوكيميائيًا مناعيًا، أكثر من الجليبنكلاميد.
الإستنتاج: يتمتع الأفوكادو فول الصويا بفاعلية حماية شبكية أكبر على إعتلال الشبكية السكري مقارنة بالجليبينكلاميد.